Energy 237 (2021) 121195

Contents lists available at ScienceDirect

Energy

journal homepage: www.elsevier.com/locate/energy

Resilience maximization through mobile battery storage and diesel DG in integrated electrical and heating networks

Hasan Mehrjerdi [a], Sajad Mahdavi [b], Reza Hemmati [b, *]

[a] Electrical Engineering Department, Qatar University, Doha, Qatar
[b] Department of Electrical Engineering, Kermanshah University of Technology, Kermanshah, Iran

ARTICLE INFO

Article history:
Received 5 December 2020
Received in revised form
24 April 2021
Accepted 7 June 2021
Available online 11 June 2021

Keywords:
Combined heat and power
Mobile battery storage
Mobile diesel generator
Pricewise linearization
Resilience
Self-adequacy

ABSTRACT

The purpose of this paper is to demonstrate the impacts of mobile battery and diesel DG in integrated electrical-heating networks for promoting the resilience, self-adequacy, load restoration, power quality as well as reducing the load shedding and operational cost. The case study is IEEE 33-bus electrical system with both the electrical and heating demands. Several buses of the grid are integrated with combined heat and power (CHP). The battery is moved between the buses hourly and the diesel DG is moved seasonally. The transfer time between origin and destination buses is considered in the given model. The electric network feeds three regions (i.e., three different loading patterns) including residential, industrial and agricultural areas where the major activity of the industrial loads is at night due to low energy price and the major activity of the agricultural loads is in the spring and summer. The outage of electricity and natural gas (NG) are two faults that are imposed on the network in order to evaluate the resilience and load restoration. The demand response program (DRP) is included in the model. Both the active and reactive powers are considered for battery, diesel DG and CHP. Several cases are simulated, studied and compared like fixed, mobile and mixed fixed-mobile locations for energy resources. The simulation results show that the proposed model reduces the total annual cost by 16.5% while the other costs such as purchased energy, NG and losses are reduced by 16.5%, 22.9% and 21.5%, respectively. The self-adequacy of network is increased by 2.5 h and the electrical-heating load restorations are increased by 36% and 38%, respectively.

1. Introduction

1.1. Motivations of this work

Nowadays, the industry and manufacturing tightly depend on the electrical grid functionality and such point makes the electric power industry one of the most important infrastructure in the world. Therefore, the safe and resilient operation of power systems under extreme weather or attacks is very important. Such events can impose heavy damages to the governments, e.g., on September 28, 2003, falling a tree on one main grid line not only resulted in blackout of 56 million peoples in Italy and Switzerland but also it left 1.2 billion euro damage [1]. On December 23, 2013, the cyber-attack to several energy distribution companies caused the power outage of 230 thousand for 6 h in Ukraine [2]. The storm in South Australia on September 28, 2016 cut off power of 850 thousand customers and even 456 MW wind extra generation could not avoid the voltage collapse [3]. Therefore, the natural disasters and cyber-attack are the serious hazards for electrical grids and the damage is often significant [4].

The multi carrier energy (MCE) systems with combination of electrical and NG networks in order to generate electricity, heating and cooling at the same time. Such systems are one of the efficient methods to enhance resilience, reduction of energy costs and decreasing CO_2 and greenhouse gas emissions in electric power systems [5–7]. The combined heat and power (CHP) unit [8], electrical and absorption chillers [9], power to gas (P2G) technology [10], boiler [11], different types of storages such as stationary battery [12], heating [13], cooling [14], NG [15], hydrogen [16] and carbon dioxide [17] are common equipment in MCE systems.

In recent years, the modelling and simulation of such facilities have been discussed in the literatures but the mobile resources

* Corresponding author. Department of Electrical Engineering, Kermanshah University of Technology, Kermanshah, P.O.Box: 6715685420, Iran.
E-mail addresses: Hasan.mehrjerdi@qu.edu.qa (H. Mehrjerdi), smahdavik@gmail.com (S. Mahdavi), r.hemmati@kut.ac.ir (R. Hemmati).

https://doi.org/10.1016/j.energy.2021.121195
0360-5442/

Nomenclature

Indices and sets

i,j	Index of network buses
f, F	Index and set of faults
h, h'	Index of heating buses
l	Index of piecewise lines for linearization
NB, NH	Set of electrical and heating buses
se, SE	Index and set of seasons
s, SC	Index and set of scenarios
t, t', T	Index and set of time periods
ψ	Set of buses for mobile diesel DG
Ω	Set of buses for mobile battery
χ	Set of candidate buses for demand response program (shiftable loads)

Parameters

BM	Big digit in big-m inequalities
D_{se}^{f}	Number of days in fault *f* and season *se*
E^{ini}, E^{max}, E^{min}	Initial, maximum and minimum energy of battery (kWh)
G_{ij}, B_{ij}	Conductance and susceptance of line (p.u.)
H_{bo}^{max}	Maximum generated heating power of boiler (kW)
H_{chp}^{A} ,H_{chp}^{B}, H_{chp}^{C} ,H_{chp}^{D}	Heating power related to CHP feasible region (kW)
P_{chp}^{A} ,P_{chp}^{B}, P_{chp}^{C} ,P_{chp}^{D}	Active power related to CHP feasible region (kW)
P_{ch}^{max}, P_{dis}^{max}	Maximum charging-discharging power rate of battery (kW)
PD,QD,HD	Active, reactive and heating power demand (kW, kVar)
PV, PW	Active power of solar and wind unit (kW)
Pr_{sh}, Pr_{st}	Start-up and shut-down price of CHP ($)
Pr_{p}, Pr_{q}	Price of active and reactive purchased energy ($/kWh, $/kVarh)
Pr_{pdg}, Pr_{qdg}	Price of active and reactive generation power of diesel DG ($/kWh, $/kVarh)
Pr_{drp}, Pr_{drq}	Price of active and reactive shifted power by demand response program ($/kW, $/kVar)
Pr_{pshed}, Pr_{qshed}	Price of active and reactive curtailed power by load shedding program ($/kW, $/kVar)
Pr_{hshed}	Price of heating curtailed power by load shedding program($/kW)
Pro_{s}	Probability of scenario
L	Number of all piecewise lines for linearization
NG_{tank}^{ini}	Initial NG in tank storage (kg)
NG_{rate}^{max}, NG_{cap}^{max}	Maximum NG flow rate (kg/h) and tank storage (kg)
S_{chp}^{A}, S_{line}^{max} ,S_{MB}^{max}, S_{DG}^{max}	Maximum capacity of CHP, line, mobile battery storage and diesel DG (kVA)
$TT^{i,j}$	Transfer time of mobile battery between bus i and j (hour)
ΔT	Duration of time interval (hour)
β_{NG}	Conversion coefficient of kWh to kg for NG (kg/kWh)
θ^{max}	Maximum angle difference between buses of network (Radian)
η_{P}^{chp} ,η_{H}^{chp}, η_{H}^{bo}	Active and heating efficiency of CHP and boiler (%)
η^{ch},η^{dis}	Charging and discharging efficiency of mobile battery (%)
γ	Shiftable load factor (%)
$\xi_{loss}^{hh'}$	Heating losses factor for heating lines between buses h and h' (%)

Binary variables

u, x	Auxiliary variables for modelling the battery charging/discharging and CHP
z, κ	Auxiliary variables for modelling the movement of battery and diesel DG
δ, λ	Auxiliary variables for linearization of θ^2

Continuous variables

$C_{CHP}^{st\&sh}$	Summation of start-up and shut-down annual cost of CHP ($/year)
$C_{st}^{se,f,t}$,$C_{sh}^{se,f,t}$	Start-up and shut-down cost of CHP ($)
$C_{in}^{p,q}$	Cost of active and reactive purchased power from network ($/year)
C_{loss}	Cost of active and reactive losses ($/year)
C_{DG}	Operational cost of mobile diesel DG ($/year)
C_{DR}	Incentive cost for shiftable loads in demand response program ($/year)
C_{in}^{NG}	Cost of purchased NG ($/year)
C_{shed}^{elec}, C_{shed}^{heat}	Electrical and heating load shedding costs ($/year)
DRP_{up}, DRP_{down}	Added or deducted active demand related to shiftable loads (kW)
DRQ_{up}, DRQ_{down}	Added or deducted reactive demand related to shiftable loads (kW)
E	Stored energy in mobile battery storage (kWh)
$HF_{hh'}$	Heating flow between buses h and h' (kW)
H_{bo}	Heating power of boiler (kW)
$NGC_{chp,bo}$	NG consumption by CHP and boiler (kg)
NG_{in}	The purchased NG from network (kg)
NG_{tank}	NG flow rate for tank storage (kg/h)
NG_{cap}	Stored NG in tank storage (kg)
P_{chp}, Q_{chp}, H_{chp}	Active, reactive and heating power of CHP (kw)
P_{DR}, Q_{DR}	The new active and reactive loads after applying the demand response program (kW)
P_{in}, Q_{in}	Active and reactive input power to network (kW, kVar)
P_{ch}, P_{dis}	Charging and discharging power of mobile battery (kW)
P_{DG}, Q_{DG}	Active and reactive power of mobile diesel DG (kW, kVar)
P_{ij}, Q_{ij}	Active and reactive power between buses i and j (kW, kVar)
$P_{loss}^{i,j}$, $Q_{loss}^{i,j}$	Active and reactive losses between buses i and j (kW, kVar)
V_{i}, θ_{i}	Amplitude and angle of voltage (p.u., radian)
ω_{elec}, ω_{heat}	load shedding coefficient (%)
$\Delta\theta_{ij}$, θ_{ij}^{+}, θ_{ij}^{-}	Auxiliary variables for linearization of θ^2

have not been adequately studied especially for energy resilience improvement in MCE systems. The mobile energy resources such as mobile battery and mobile emergency diesel generator have great potential to promote the resilience and flexibility of network [18]. The distribution systems due to the radial topology and limitation of backup capacity can be very vulnerable against the natural disasters and physical-cyber attracts. The emerging technologies such as mobile batteries (installed on truck or train and called storage-on-wheels) [19] are therefore hopeful in distribution grids. These mobile batteries are available in different power ranges such as 100, 1000 and 5000 kW [20], e.g., the 500kW/1000 kWh mobile battery storage is applied for peak shaving in china [21]. Authors in Ref. [22] model a mobile energy generation including PV panel array, fuel cell stack, hydrogen tank and battery pack that are mounted on container. The problem is formulated as a mix integer planning in order to maximize profit of mobile energy generation system fleet.

Over the last few years, the stationary batteries have been broadly investigated in literature but despite of their advantages they have some disadvantages: (i) during faults and events the faulty area including storage system may be separated from the grid while the mobile storage can be transported to other locations, (ii) the predefined and fixed charging-discharging operation pattern of stationary battery may be in conflict with the future load demand, (iii) the stationary battery is not efficient during off-peak seasons and it may be switched off for one season, such battery can be transported to the other areas that are under on-peak load demand, (iv) the electricity generation by PV solar system is minimum in the cloudy days or weeks and the stationary battery is charged insufficient but the mobile battery can be moved to the area with higher solar irradiation. Therefore, the mobile batteries have maneuvering power more than stationary ones. Some advantages of mobile batteries investigated by researchers are listed and referenced as follows: reduction of lines congestion and network operation costs [23], reduction of wind power curtailment [24], voltage regulation and power quality improvement [25], frequency regulation [26], enhancing the resilience [27], energy transport between different points of network and increasing the network flexibility [28], enhancing reliability [29], reduction of charging/discharging cycles of stationary battery [30], network expansion deferral and reduction of reinforcement cost [31], minimization the greenhouse gases [32].

1.2. Literature survey

The wind power penetration to the grids is often limited by transmission line thermal capacity or heavy costs of lines reinforcement, e.g., more than 4000 GWh of wind energy was curtailed in 2015 in Germany [33]. The authors in Ref. [33] have simulated a wind power plant in Germany with 134 GWh curtailed energy during 32% of time in 2017. The mobile battery can be charged by the curtailed energy and deliver it as backup power for off-grid applications such as festivals and concerts as well as grid maintenance. In literatures, the modelling of battery movement is based on the specific method such as train or truck that reduces the model flexibility because by changing the movement method, the problem should be re-arranged. In order to address this problem, a new optimal scheduling of mobile battery is presented by Ref. [34], in the given mode, the modelling is independent of transfer method and the charging/discharging scheduling of battery is optimized subject to technical constraints and transfer time between buses.

The distribution network resilience is based on three parameters including prevention, recovery and survivability. The mobile power resources are effective responsible resources to recovery and survivability of network [18]. A two stage framework for resilience strengthen by mobile battery and mobile diesel DG is presented by Ref. [18]. The first stage is before the event and the resources are pre-positioned and the second stage is after the event that the resources are dispatched dynamically for load restoration. The model improves both the recovery and survivability. The system reformation before occurrence of natural disaster is also effective to prevent the excessive destruction and increasing system preparedness and such model can enhance the survivability and restoration capability of distribution system [27].

One of the important benefits of mobile battery is to revive the isolated areas from blackout at fault time. The impact of mobile battery to recovery the blackout in distribution network is shown by Fig. 1. As seen in part (a), occurrence of a fault in bus 2 leads to blackout in bus 6–11 because there is not any power generation in this area, but in part (b), the battery that is installed on a truck restores this area. Therefore, the load restoration is increased by mobile battery or mobile diesel DG [35]. Consideration of traffic time on road networks as traffic factor in the mathematical modelling can increase the model accuracy. An open capacity expansion model of power system with mobile battery is proposed by Ref. [36], where in order to provide an actual planning, the geographic information and traffic routes are considered. The authors in Ref. [37] present a two level framework with pre-positioning and real-time allocation and consideration of traffic model in order to restore the critical loads by system formation. Simulation results show how much the traffic issue is effective to increase the model accuracy, especially in real-time allocation level. Assessment of mobile battery to promote the network reliability with consideration of traffic factor is proposed by Ref. [29] and it is shown that at fault time, the mobile battery can move towards the isolated areas and restore the critical loads. The seasonal movement of mobile battery as well as the coordinated dispatch of mobile and stationary battery is proposed by Ref. [31] and the results are reliability enhancement, reduction of losses, energy and reinforcement costs decrement. Sizing and planning of mobile battery energy storage in order to maximize the company profit, energy arbitrage, voltage regulation and power losses minimization is proposed by Ref. [38]. The adopted technique is based on PSO algorithm and mixed-integer convex planning. The mobile charging station (MCS) as one of the factors of sustainable development can be utilized for

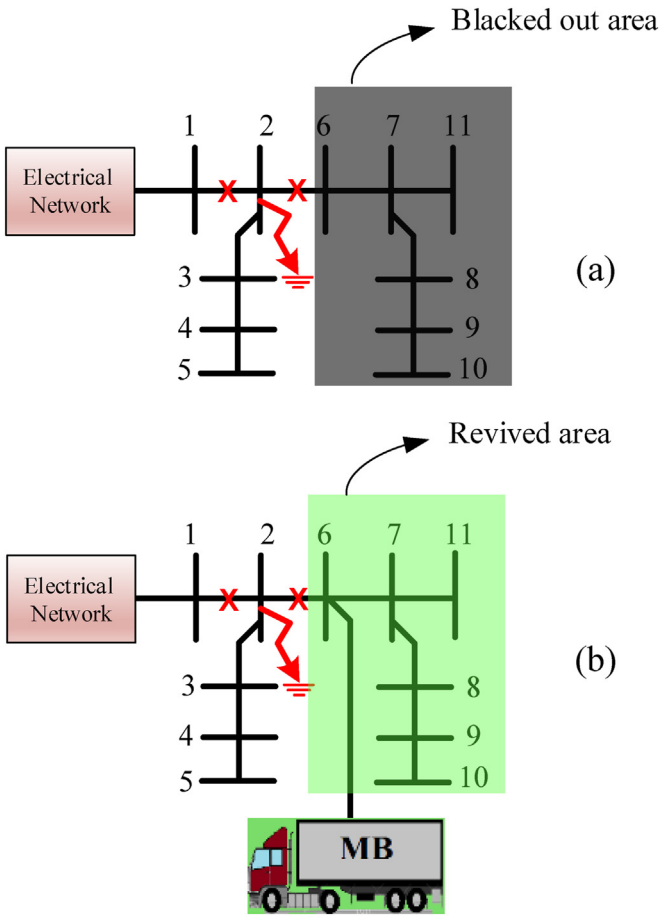

Fig. 1. Distribution network, (a) without (b) with mobile battery.

minimizing electric vehicle (EV) charging cost [39] and it proves that MCSs are very effective for reducing cost, network voltage drop and charging queue.

1.3. Contributions of the given model

According to the literature review, there are many outstanding aspects about mobile energy resources as well as hybrid mobile-stationary combinations. This paper aims to address these issues all together in one compressive model. The developed model presents a coordination stochastic plan for mobile battery and mobile DG diesel operation in integrated electrical and heating grid. The objectives of the model are maximization of electrical-heating load restoration, network self-adequacy, resilience under faults and minimization of overall cost. The hybrid mobile-stationary model is utilized to optimize the electricity and heating flows in the integrated electrical-heating networks. The various loading areas including agricultural, industrial and residential with different seasonal and hourly loading profiles are combined with proper demand response program including critical, shiftable and curtailable loads. The reactive power is included to evaluate the voltage profile. The reactive power of CHP, mobile battery and mobile diesel DG is optimally dispatched in order to improve the voltage profile. The loads and renewables are modeled by probability distribution functions. The main contributions of the given model can be summarized as follows:

- Employment of mobile battery for enhancing load restoration in both electrical and heating networks.
- Optimal movement of disel DG (seasonally) and battery storage (hourly, based on transfer time) to minimize operational cost and improvement of electrical-heating loads restoration.
- Modelling the shiftable, curtailable, and critical loads as well as load shedding strategy in the form of demand response program.
- Both active and reactive powers and losses are incorporated in the model.
- The uncertainty behavior of all loads and renewable resources are modeled by probability distribution functions and such fluctuations are managed by stochastic programming.

2. Problem statement

The main purpose of current work is to present the coordinated optimal scheduling for mobile battery-diesel together with the other equipment. In the proposed model, the mobile battery is transferred between the buses and installed at new locations after the elapsed time or transfer time. During the transfer time, the battery is disconnected from the grid. The transfer of battery is scheduled based on hourly pattern. The mobile diesel DG is one of the other backup resources that is considered in model. The mobile diesel is transferred seasonally and it takes about 1 h in each season. As a result, the effect of transfer time in not significant against the total hours of the season and can be neglected. Both the mobile battery and diesel DG can generate active and reactive powers and may be utilized for voltage profile improvement.

The grid is divided to three areas including agricultural, industrial and residential zones and each zone supplies a various load profile. The agricultural loads are usually on peak demand during spring and summer while the industrial loads have constant load profile over all seasons. From the point of view of hourly operation, the industrial loads often use higher energy during night hours when the energy price is cheap. Both the electrical and heating loads are supplied through integrated electrical-heating grid. Some of the industrial and heating loads are signified as critical load and their energy must not be interrupted. The incentive-based demand response program (DRP) is modeled in the residential area by shiftable and curtailable loads. The curtailable loads are paid by penalty cost considering the total or partial load shedding. The

successful restoration of the curtailed loads is one of the resilience indexes considered by the developed model.

The schematic of proposed network is shown by Fig. 2. As seen in this figure, the electrical and NG networks are the main input suppliers. In current work, operation of heating network is developed by a simple, linear and static model. The Quasi dynamic interactions between electricity and heating networks as well as dynamic model of heating network considering heating losses and transfer delay in the pipe-lines can be found in Refs. [40,41]. The battery and diesel DG stations cover almost all areas of the system. The NG storage tank is very effective in reduction of cost and enhancing the load restoration under the NG shortage time periods. The boiler and CHP generate heating but the CHP produces active and reactive powers (electrical energy) besides the heating. It is noteworthy that due to CHP structure restrictions (i.e. turbine structure, input gas flow and etc.), the generated heat and power are dependent and such relationship restricts the CHP operation which is known as "feasible region". The feasible region of a typical CHP is shown in Fig. 3. According to this figure, in points A and B, the power and heat generation are maximum. In points C and D, the power and heat generation are minimum. The fuel consumption in AB and DC segments is maximum and minimum, respectively. Meanwhile, in AD segment only the power is generated while in BC segment the heat extraction is maximum.

In order to evaluate the resilience, the electricity and NG outage are imposed to network as fault in each season. The input data to model are the loads, lines, solar and wind profiles as well as the parameters related to mobile battery, diesel DG, CHP, boiler and NG tank storage. The outputs of the model are battery location at each hour, hourly charging-discharging regime of battery, diesel DG seasonally location, hourly generation of diesel, voltage of buses, active and reactive powers through the lines, energy losses, heating flow and losses, hourly generation of boiler, absorption-rejection NG flow by storage tank, CHP operation (i.e., heating, active, reactive power), load shifting and load shedding programs. The objective function is to minimize the annual operational cost subject to set of constraints such as CHP feasible region, limitation of lines flow, power balance and voltage limitations. The proposed model considers different loading and energy profiles for each season. In each season, one typical day is considered for evaluating the system. As a result, there are four different days in four seasons and each day has different loading and energy profiles. Based on such model, the seasonal operational cost is achieved by multiplying the daily operational cost by number of days in the season (e.g. 90 days). Then, all four different seasonal operational costs are added to make the final annual operational cost.

3. Mathematical formulation

The proposed model is a linear programming because it has been proven that the linear programming achieves the global optimal solution certainly but the outputs of non-linear programming are not guaranteed to be the global optimal solution and they may be the local optimal solution. In the linear models, the non-linear functions are approximated by linear equal functions and such linearization and approximations decrease the model accuracy and create some errors in the linearized model. The less linearization approximation increases the model accuracy. In the proposed model, the minimum linearization approximations are used. A simple linear model is also assumed for the heating network which creates some errors and inaccuracy in the model but such simple linear model avoids the nonlinearity in the problem resulting in a linear programming.

3.1. CHP and boiler formulation

The operation of CHP is restricted by a feasible region. The linear constraints (1) to (4) are necessary and sufficient conditions for placement of CHP operating conditions inside the polygon region, when x = 0, the output apparent power and heating of CHP are zero. It is noteworthy, these equations show the formulations related to the lines AB, BC and CD, respectively. The CHP apparent power is restricted by (5) and (6). In order to linearize (6), the hexagon approximation of a circle is used as expressed by (7) where L is number of lines piece. The approximation of a circle by an enclosed hexagon is shown in Fig. 4 and more details can be found in Ref. [42]. equation (8) expresses the heating range of boiler. Another CHP modelling based on ramp-down and ramp-up of can be found in Ref. [6] and feasible operation region modelling without using of binary variables is introduced by Ref. [40].

$$P_{chp}^{se,f,t} - P_{chp}^{A} - \frac{P_{chp}^{A} - P_{chp}^{B}}{H_{chp}^{A} - H_{chp}^{B}}\left(H_{chp}^{se,f,t} - H_{chp}^{A}\right) \le 0 \tag{1}$$

$$P_{chp}^{se,f,t} - P_{chp}^{B} - \frac{P_{chp}^{B} - P_{chp}^{C}}{H_{chp}^{B} - H_{chp}^{C}}\left(H_{chp}^{se,f,t} - H_{chp}^{C}\right) \le -\left(1 - x^{se,f,t}\right).BM \tag{2}$$

$$P_{chp}^{se,f,t} - P_{chp}^{C} - \frac{P_{chp}^{C} - P_{chp}^{D}}{H_{chp}^{C} - H_{chp}^{D}}\left(H_{chp}^{se,f,t} - H_{chp}^{D}\right) \ge -\left(1 - x^{se,f,t}\right).BM \tag{3}$$

$$0 \le H_{chp}^{se,f,t} \le H_{chp}^{B}.x^{se,f,t} \tag{4}$$

$$0 \le S_{chp}^{se,f,t} \le S_{chp}^{A}.x^{se,f,t} \tag{5}$$

$$P_{chp}^{se,f,t}\left(P_{chp}^{se,f,t}\right)^2 + \left(Q_{chp}^{se,f,t}\right)\left(P_{chp}^{se,f,t}\right)\left(P_{chp}^{se,f,t}\right)^2 + \left(Q_{chp}^{se,f,t}\right)\left(P_{chp}^{se,f,t}\right)\left(P_{chp}^{se,f,t}\right)^2 + \left(Q_{chp}^{se,f,t}\right)^2 \le \left(S_{chp}^{A}\right)^2 \tag{6}$$

$$P_{chp}^{se,f,t}.\cos\frac{(2l-1)}{L}\pi + Q_{chp}^{se,f,t}.\sin\frac{(2l-1)}{L}\pi - S_{chp}^{A}.\cos\frac{\pi}{L} \le 0 \quad \forall\, l \in \{1,2,\ldots L\} \tag{7}$$

$$0 \le H_{bo}^{se,f,s,t} \le H_{bo}^{\max} \tag{8}$$

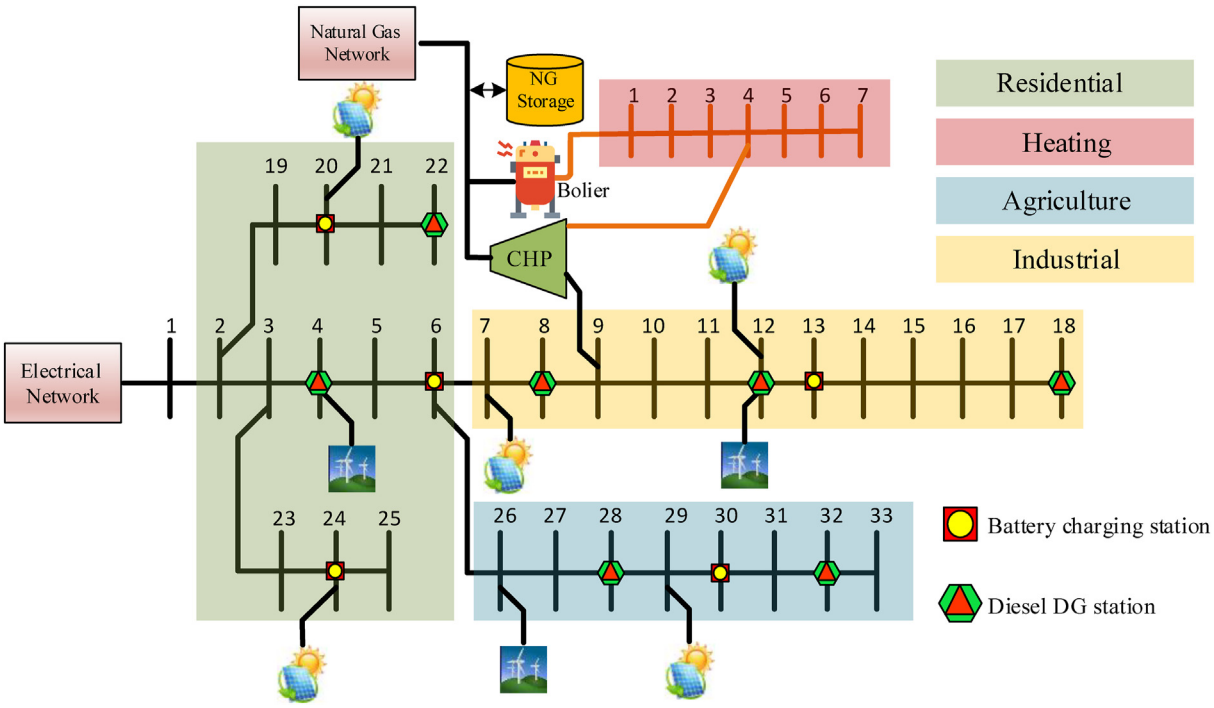

Fig. 2. Schematic of the proposed network.

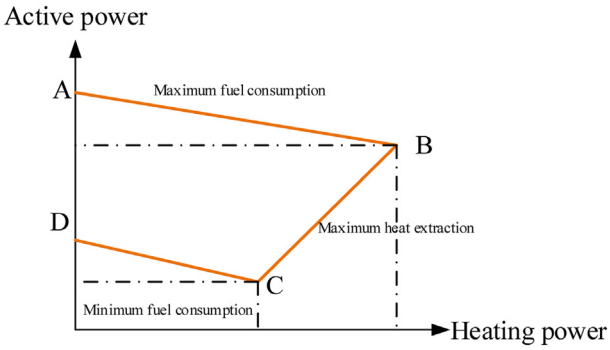

Fig. 3. Feasible region of CHP operation.

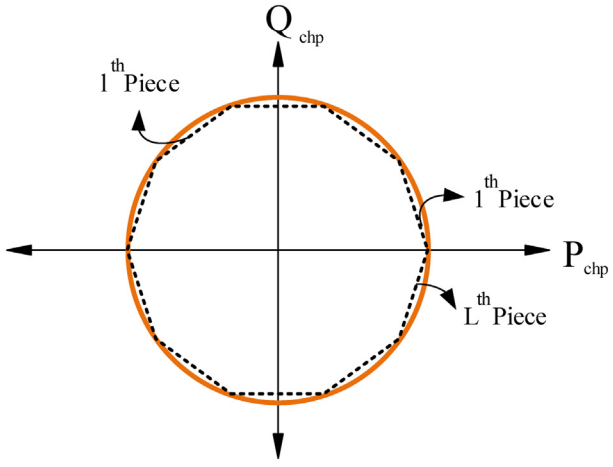

Fig. 4. Approximation of a circle by hexagon.

3.2. Mobile diesel DG operation

The hourly active and reactive power of diesel DG are formulated by (9) and (10), the $\kappa^{i,se} = 0$ means the diesel DG is not installed on bus 'i' in all days of season. As seen in (10), diesel DG can absorb or inject the reactive power. The apparent power of diesel DG is restricted by the inequality shown by (11). In this paper it is assumed that the mobile diesel DG can be installed only on one bus in each season as expressed by (12).

$$0 \le P_{DG}^{i,se,f,t} \le \kappa^{i,se}.\, S_{DG}^{\max} \quad \forall i \in \psi \tag{9}$$

$$-\kappa^{i,se}.\,S_{DG}^{\max} \le Q_{DG}^{i,se,f,t} \le \kappa^{i,se}.\,S_{DG}^{\max} \quad \forall i \in \psi \tag{10}$$

$$P_{DG}^{i,se,f,t}.\cos\frac{(2l-1)}{L}\pi + Q_{DG}^{i,se,f,t}.\sin\frac{(2l-1)}{L}\pi - S_{DG}.\cos\frac{\pi}{L} \le 0 \quad \forall\, l \in \{1,2,\ldots L\}\,,\; i \in \psi \tag{11}$$

$$\sum_{i\in\Psi}\kappa^{i,se} = 1 \tag{12}$$

3.3. Mobile battery formulation

The hourly stored energy in mobile battery is defined by (13) and (14). The stored energy at end of time period must be equal to the beginning of the period and such balance is expressed by (15). The battery energy is limited by (16) in each time interval. The charging and discharging states of battery must not be happened simultaneous as defined by (17) and (18). The apparent power of battery is restricted by (19). The battery model comprises both active and reactive powers and it is able to absorb or inject reactive power.

$$E^{se,f,t} = E^{ini} + \sum_{i\in\Omega}\left(P_{ch}^{i,se,f,t}\,.\,\eta^{ch} - P_{dis}^{i,se,f,t} \Big/ \eta^{dis}\right)\Delta T \quad \forall t = 1 \tag{13}$$

$$E^{se,f,t} = E^{se,f,t-1} + \sum_{i\in\Omega}\left(P_{ch}^{i,se,f,t}\,.\,\eta^{ch} - P_{dis}^{i,se,f,t} \Big/ \eta^{dis}\right)\Delta T \quad \forall t \ne 1 \tag{14}$$

$$E^{se,f,t} = E^{ini} \quad \forall\, t = t_T \tag{15}$$

$$E^{\min} \le E^{se,f,t} \le E^{\max} \tag{16}$$

$$0 \le P_{ch}^{i,se,f,t} \le P_{ch}^{\max}\,.\,u^{i,se,f,t} \quad \forall\, i \in \Omega \tag{17}$$

$$0 \le P_{dis}^{i,se,f,t} \le P_{dis}^{\max}\,.\left(1 - u^{i,se,f,t}\right) \quad \forall\, i \in \Omega \tag{18}$$

$$\left(P_{ch}^{i,se,f,t} - P_{dis}^{i,se,f,t}\right).\cos\frac{(2l-1)}{L}\pi + Q_{MB}^{i,se,f,t}.\sin\frac{(2l-1)}{L}\pi - S_{MB}^{\max}.\cos\frac{\pi}{L} \le 0 \;\forall\, l \in \{1,2,\ldots L\}\,,\; i \in \Omega \tag{19}$$

In this paper, it is assumed that the battery storage can be transported hourly. The battery is not installed when Z = 0 and it can be installed only on one or none of buses at each time interval. These points are expressed by (20)-(22). Similar to energy balance, battery location in end of period must be equal to beginning of period which is modeled in (23). In transfer time between buses i and j, battery must not be connected to network, this problem is guaranteed by (24).

$$0 \le P_{ch}^{i,se,f,t} \le P_{ch}^{\max}\,.\,Z^{i,se,f,t} \quad \forall\, i \in \Omega \tag{20}$$

$$0 \le P_{dis}^{i,se,f,t} \le P_{dis}^{\max}\,.\,Z^{i,se,f,t} \quad \forall\, i \in \Omega \tag{21}$$

$$\sum_{i\in\Omega} Z^{i,se,f,t} \le 1 \tag{22}$$

$$Z^{i,se,f,t_1} = Z^{i,se,f,t_T} \quad \forall\, i \in \Omega \tag{23}$$

$$Z^{i,se,f,t} + Z^{j,se,f,t'} \le 1 \quad \forall\, t' \in \left[t+1\,,\; t+TT^{i,j}\right] \quad,\quad i,j \in \Omega\,,\; i \ne j \tag{24}$$

3.4. NG consumption and storage

The NG consumption by CHP and boiler is modeled by (25) and the purchased NG is defined by (26). The hourly stored NG in tank storage is modeled by (27) and (28). The NG flow rate is restricted by (29), where the negative and positive signs means eject and absorb of tank, respectively. The stored NG at end of time-period must be equal to the beginning of the period and such balance is expressed by (30). The stored NG is limited by (31) in each time interval.

$$NGC_{chp,bo}^{se,f,s,t} = \left(P_{chp}^{se,f,t} \Big/ \eta_P^{chp} + H_{chp}^{se,f,t} \Big/ \eta_H^{chp} + H_{bo}^{se,f,s,t} \Big/ \eta_H^{bo}\right).\,\beta_{NG} \tag{25}$$

$$NG_{in}^{se,f,s,t} = NGC_{chp,bo}^{se,f,s,t} + NG_{\tan k}^{se,f,t} \tag{26}$$

$$NG_{cap}^{se,f,t} = NG_{\tan k}^{ini} + NG_{\tan k}^{se,f,t}\,.\,\Delta t \quad \forall\, t = 1 \tag{27}$$

$$NG_{cap}^{se,f,t} = NG_{\tan k}^{se,f,t-1} + NG_{\tan k}^{se,f,t}\,.\,\Delta t \quad \forall\, t \ne 1 \tag{28}$$

$$-NG_{rate}^{\max} \le NG_{\tan k}^{se,f,t} \le NG_{rate}^{\max} \tag{29}$$

$$NG_{cap}^{se,f,t} = NG_{\tan k}^{ini} \quad \forall\, t = t_T \tag{30}$$

$$NG_{cap}^{\min} \le NG_{cap}^{se,f,t} \le NG_{cap}^{\max} \tag{31}$$

3.5. Demand response program

The demand response is one of the most important flexible tools in order to manage the loads and energy costs [32,43,44]. In this paper, an incentive-based demand response is implemented through shifting the load demand to the next time periods. The level of shiftable load at each time is expressed by (32) and (33). The reduced load must be added in the next time-periods which means sum of the load reduction must be equal to sum of the load increment as shown by (34). The finally amount of demand is defined by (35). The DRP for reactive part of load is calculated by (36) to (38).

$$DRP_{up}^{i,sef,s,t} \le \gamma \,.\, PD^{i,sef,s,t} \quad \forall\, i \in \chi \tag{32}$$

$$DRP_{down}^{i,sef,s,t} \le \gamma \,.\, PD^{i,sef,s,t} \quad \forall\, i \in \chi \tag{33}$$

$$\sum_{t \in T} DRP_{up}^{i,sef,s,t} = \sum_{t \in T} DRP_{down}^{i,sef,s,t} \quad \forall\, i \in \chi \tag{34}$$

$$PD_{DR}^{i,sef,s,t} = PD^{i,sef,s,t} + DRP_{up}^{i,sef,s,t} - DRP_{down}^{i,sef,s,t} \quad \forall\, i \in \chi \tag{35}$$

$$DRQ_{up}^{i,sef,s,t} \le \gamma \,.\, QD^{i,sef,s,t} \quad \forall\, i \in \chi \tag{36}$$

$$DRQ_{down}^{i,sef,s,t} \le \gamma \,.\, DQ^{i,sef,s,t} \quad \forall\, i \in \chi \tag{37}$$

$$\sum_{t \in T} DRQ_{up}^{i,sef,s,t} = \sum_{t \in T} DRQ_{down}^{i,sef,s,t} \quad \forall\, i \in \chi \tag{38}$$

$$QD_{DR}^{i,sef,s,t} = QD^{i,sef,s,t} + DRQ_{up}^{i,sef,s,t} - DRQ_{down}^{i,sef,s,t} \quad \forall\, i \in \chi \tag{39}$$

3.6. Linearization of power flow

The active and reactive power flow between two buses are calculated by nonlinear equations (40) and (41). The relationship shown by (42) is applied for linearization of them. It is noteworthy θ_{ij} is very small and the Taylor series is used. Therefore, (43) and (44) are obtained by placement of (42) in (40)-(41) and elimination of very small elements. The active and reactive losses of the line are calculated by (45) and (46), details of this method can be found [45].

$$P_{ij} = V_i^2 G_{ij} - V_i V_j (G_{ij} \cos\theta_{ij} + B_{ij} \sin\theta_{ij}) \tag{40}$$

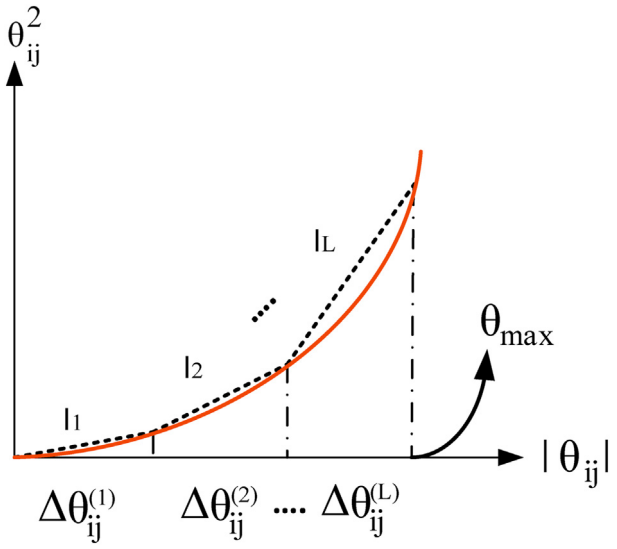

Fig. 5. Piecewise linear approximation of second order curve.

$$Q_{ij} = -V_i^2 B_{ij} - V_i V_j (G_{ij} \sin\theta_{ij} - B_{ij} \cos\theta_{ij}) \tag{41}$$

$$V_i = 1 + \Delta V_i \quad ,\ \sin\theta_{ij} = \theta_{ij},\ \cos\theta_{ij} = 1 - \theta_{ij}^2/2\ ,\ \theta_{ij} = \theta_i - \theta_j \tag{42}$$

$$P_{ij}^{sef,s,t} = G_{ij}\left(\Delta V_i^{sef,s,t} - \Delta V_j^{sef,s,t}\right) - B_{ij}\theta_{ij}^{sef,s,t} + G_{ij}\left(\theta_{ij}^{sef,s,t}\right)^2 \Big/ 2 \tag{43}$$

$$Q_{ij}^{sef,s,t} = -B_{ij}\left(\Delta V_i^{sef,s,t} - \Delta V_j^{sef,s,t}\right) - G_{ij}\theta_{ij}^{sef,s,t} - B_{ij}\left(\theta_{ij}^{sef,s,t}\right)^2 \Big/ 2 \tag{44}$$

$$P_{loss}^{i,j,sef,s,t} = G_{ij}\left(\theta_{ij}^{sef,s,t}\right)^2 \tag{45}$$

$$Q_{loss}^{i,j,sef,s,t} = -B_{ij}\left(\theta_{ij}^{sef,s,t}\right)^2 \tag{46}$$

As seen in above equations, θ^2 is a nonlinear part and piecewise

linear approximation of second order curve is applied to linearize this term. The constraints of this approximation are presented by (47) to (54). Extra explanations and more details can be found in Ref. [46]. The piecewise linear approximation of second order curve is shown by Fig. 5 [46,47].

$$\left(\theta_{ij}^{se,f,s,t}\right)^2 = \sum_{l\in L}(2l-1)\Delta\theta_{ij}^{l,se,f,s,t} \cdot \theta^{\max} \Big/ L \tag{47}$$

$$\theta_{ij}^{se,f,s,t} = \theta_{ij}^{se,f,s,t^+} - \theta_{ij}^{se,f,s,t^-} \tag{48}$$

$$\sum_{l\in L}\Delta\theta_{ij}^{l,se,f,s,t} = \theta_{ij}^{se,f,s,t^+} + \theta_{ij}^{se,f,s,t^-} \tag{49}$$

$$\theta_{ij}^{se,f,s,t^+} \le \delta_{ij}^{se,f,s,t}\theta^{\max} \tag{50}$$

$$\theta_{ij}^{se,f,s,t^-} \le \left(1-\delta_{ij}^{se,f,s,t}\right)\theta^{\max} \tag{51}$$

$$\lambda_{ij}^{l,se,f,s,t} \cdot \theta^{\max} \Big/ L_{\max} \le \Delta\theta_{ij}^{l,se,f,s,t} \le \theta^{\max} \Big/ L \quad \forall\ l=1 \tag{52}$$

$$\lambda_{ij}^{l,se,f,s,t} \cdot \theta^{\max} \Big/ L_{\max} \le \Delta\theta_{ij}^{l,se,f,s,t} \le \lambda_{ij}^{l-1,se,f,s,t} \cdot \theta^{\max} \Big/ L \quad \forall\ 1<l<L \tag{53}$$

$$0 \le \Delta\theta_{ij}^{l,se,f,s,t} \le \lambda_{ij}^{l-1,se,f,s,t} \cdot \theta^{\max} \Big/ L \quad \forall\ l=L \tag{54}$$

3.7. Electrical and heating power balance

The active and reactive power balance for both types of buses, participant and non-participant in demand response program, are calculated by (55) and (56). For the buses that participate in the load shedding program, ω_{elec} is between 0 and 1 and ω_{elec} is equal to 1 for critical loads.

$$\begin{aligned} &PV^{se,f,s,t} + PW^{se,f,s,t} + P_{DG}^{i,se,f,t} + \left(P_{dis}^{i,se,f,t} - P_{ch}^{i,se,f,t}\right) \\ &+P_{chp}^{se,f,t} - \sum P_{ij}^{se,f,s,t}\ {}^{j\in NB}_{j\ne i} = \begin{cases} PD_{DR}^{i,se,f,s,t} & \forall\ i\in\chi \\ \omega_{elec}^{i,se,f,s,t} \cdot PD^{i,se,f,s,t} & \forall i\notin\chi \end{cases} \end{aligned} \tag{55}$$

$$\begin{aligned} &Q_{DG}^{i,se,f,t} + Q_{MB}^{i,se,f,t} + Q_{chp}^{se,f,t} - \sum Q_{ij}^{se,f,s,t}\ {}^{j\in NB}_{j\ne i} \\ &= \begin{cases} QD_{DR}^{i,se,f,s,t} & \forall\ i\in\chi \\ \omega_{elec}^{i,se,f,s,t} \cdot QD^{i,se,f,s,t} & \forall i\notin\chi \end{cases} \end{aligned} \tag{56}$$

The heating power balance in buses of heating network is expressed by (57), where $0<\omega_{heat}<1$ for buses that participant in load shedding program and ω_{heat} is equal to 1 for critical loads. The heating losses in the pipes is modeled by (58). The accurate model of heating losses considering transfer delay is presented by Ref. [40].

$$\begin{aligned} &H_{bo}^{se,f,s,t} + H_{chp}^{se,f,t} - \sum_{\substack{h'\in NH \\ h'\ne h}} HF_{h'h}^{se,f,s,t} \\ &= \omega_{heat}^{h,se,f,s,t} \cdot HD^{h,se,f,s,t} \quad \forall\ h\in NH \end{aligned} \tag{57}$$

$$HF_{h'h}^{se,f,s,t} \Big/ HF_{hh'}^{se,f,s,t} = \zeta_{loss}^{hh'} \tag{58}$$

3.8. Economic terms and objective function

The start-up and shut-down of CHP cause the cost to system. The optimization of this terms therefore increases the accuracy of the model which is calculated by (59) and (60(, It is noteworthy C_{st} and C_{sh} are positive variables. Total operation cost of CHP as a second order equation is modeled by Ref. [40]. The expected value of purchased NG, active power and reactive power are calculated by (61) to (62). The expected value of losses costs is modeled by (63). The operation cost of mobile diesel DG (fuel cost for active power generation) is modeled in (64). In this paper, the DRP is based of incentive pay to participant loads and the expected value of this cost is formulated by (65). According to this relationship, the incentive cost for both of active and reactive part of the load is considered. The expected value of penalty cost for both of the electrical and heating loads that have participated in the load shedding program are calculated by (66) and (67). Finally, the objective function is summation of all of network costs consist of (60) to (67) that must be minimized by optimization algorithm. The objective function is expressed by (68).

$$\begin{aligned} C_{sh}^{se,f,t} &\ge \Pr_{sh} \cdot \left(x^{se,f,t-1} - x^{se,f,t}\right) \quad \forall\ t\ne 1 \\ C_{st}^{se,f,t} &\ge \Pr_{st} \cdot \left(x^{se,f,t} - x^{se,f,t-1}\right) \quad \forall\ t\ne 1 \\ C_{sh}^{se,f,t} &\ge \Pr_{sh} \cdot \left(x^{se,f,T} - x^{se,f,t}\right) \quad \forall\ t=1 \\ C_{st}^{se,f,t} &\ge \Pr_{st} \cdot \left(x^{se,f,t} - x^{se,f,T}\right) \quad \forall\ t=1 \end{aligned} \tag{59}$$

$$C_{CHP}^{st\&sh} = \sum_{se\in SE}\left(\sum_{se} D^f \left(\sum_{t\in T} C_{st}^{se,f,t} + C_{sh}^{se,f,t}\right)\right) \tag{60}$$

$$C_{in}^{NG} = \sum_{se\in SE}\left(\sum_{f\in F} D_{se}^{f}\left(\sum_{s\in SC}\sum_{t\in T}\beta_{NG}^{-1}.NG_{in}^{se,f,s,t}.pr_{NG}^{se,t}\,\Delta T.pro_s\right)\right) \tag{61}$$

$$C_{in}^{p,q} = \sum_{se\in 1}\left(\sum_{f\in F} D_{se}^{f}\left(\sum_{s\in SC}\left(\sum_{t\in T} P_{in}^{se,f,s,t}.pr_{p}^{se,t} + Q_{in}^{se,f,s,t}.pr_{q}^{se,t}\right)\Delta T.pro_s\right)\right) \tag{62}$$

$$C_{loss} = \sum_{se\in SE}\left(\sum_{f\in F} D_{se}^{f}\left(\sum_{s\in SC}\left(\sum_{t\in T}\frac{1}{2}\sum_{i\in NB}\sum_{\substack{j\in NB\\ j\neq i}}\begin{pmatrix}P_{loss}^{i,j,se,f,s,t}.pr_{p}^{se,t}+\\ Q_{loss}^{i,j,se,f,s,t}.pr_{q}^{se,t}\end{pmatrix}.\Delta T\right).pro_s\right)\right) \tag{63}$$

$$C_{DG} = \sum_{se\in SE}\left(\sum_{f\in F} D_{se}^{f}\left(\sum_{t\in T}\sum_{i\in \Psi}\left(P_{DG}^{i,se,f,s,t}.pr_{pdg}\right)\right)\right) \tag{64}$$

$$C_{DR} = \sum_{se\in SE}\left(\sum_{f\in F} D_{se}^{f}\left(\sum_{s\in SC}\left(\sum_{t\in T}\sum_{i\in \chi}\left(\begin{pmatrix}\left(DRP_{up}^{i,se,f,s,t}+DRP_{down}^{i,se,f,s,t}\right).pr_{drp}^{se,f,s,t}+\\ \left(DRQ_{up}^{i,se,f,s,t}+DRQ_{down}^{i,se,f,s,t}\right).pr_{drq}^{se,f,s,t}\end{pmatrix}\right).pro_s\right)\right)\right) \tag{65}$$

$$C_{elec}^{shed} = \sum_{se\in SE}\left(\sum_{f\in F} D_{se}^{f}\left(\sum_{s\in SC}\left(\sum_{t\in T}\sum_{\substack{i\in NB\\ i\neq \chi}}\left(\left(\times\left(1-\omega_{elec}^{i,se,f,s,t}\right)PD^{i,se,f,s,t}\right)pr_{pshed}^{se,f,s,t}\right).pro_s\right)\right)\right) \tag{66}$$

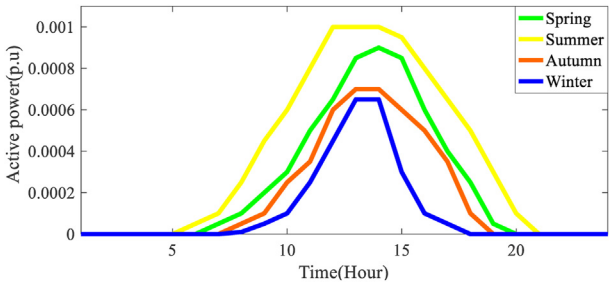

Fig. 6. Generated power of solar PV in four seasons.

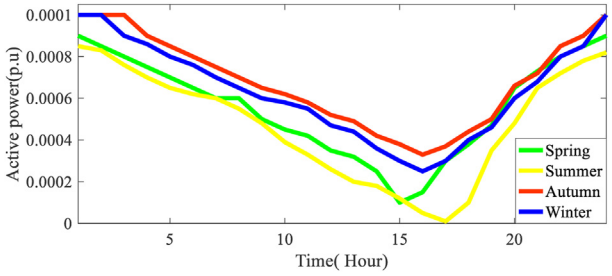

Fig. 7. Generated power of wind unit in four seasons.

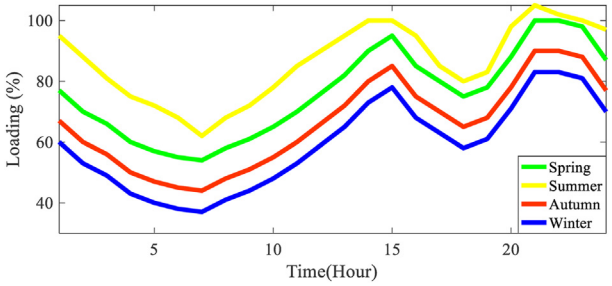

Fig. 8. Residential loads profile in four seasons.

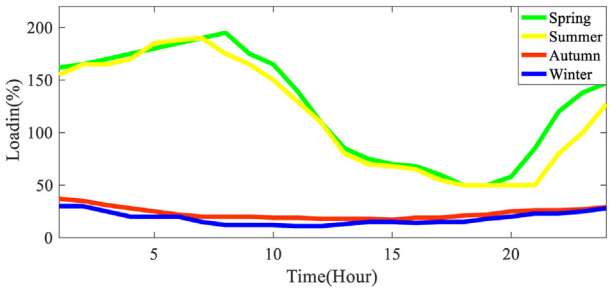

Fig. 9. Agricultural loads profile in four seasons.

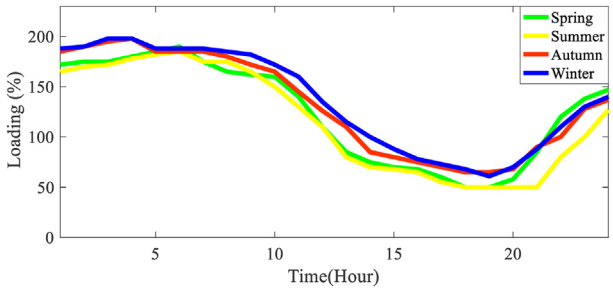

Fig. 10. Industrial loads profile in four seasons.

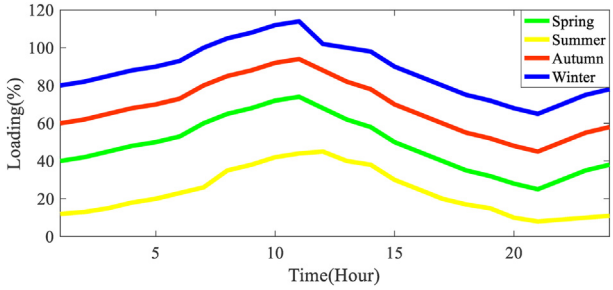

Fig. 11. Heating loads profile in four seasons.

$$C_{heat}^{shed} = \sum_{se\in SE}\left(\sum_{f\in F} D_{se}^{f}\left(\sum_{s\in SC}\left(\sum_{t\in Th}\sum_{\in NH}\left(\left(\times\left(1-\omega_{heat}^{h,se,f,s,t}\right) HD^{h,se,f,s,t}\right) pr_{hshed}^{se,f,s,t}\right)\right).pro_s\right)\right) \quad (67)$$

$$Objective\ function = C_{CHP}^{st\&sh} + C_{in}^{NG} + C_{in}^{p,q} + C_{loss} + C_{DG} + C_{DR} + C_{elec}^{shed} + C_{heat}^{shed} \quad (68)$$

4. Case study

The modified IEEE 33 bus distribution system is employed as case study. The lines and loads data of the grid can be found in Ref. [48]. In addition, the 7-bus heating radial distribution network is considered as a paralleled test system. The schematic of the proposed network with location of CHP, boiler, NG tank storage, wind and solar PV units, as well as the mobile battery and diesel DG stations is shown by Fig. 2. The electrical and NG networks are the main resources to supply the electrical and heating loads. The CHP consumes the NG and generates active-reactive and heating powers, for this reason, the CHP is a bridge between both of electrical and heating networks. The boiler is the other source of heating generation. The wind, solar PV and all loads are considered as uncertain parameters that are modeled by discrete Gaussian probability distribution functions (PDF). Each uncertain parameter follows a PDF with known mean and standard deviation. The standard deviation of uncertain parameters is considered by 10% and mean of these parameters is shown by Figs. 6–11. The PDF related to each uncertain parameter is approximated by 3 steps (discrete Gaussian PDF) that are determined as α, β, δ with probability equal to 0.06, 0.9 and 0.04, respectively. The β is equal to mean and α-δ are equal to 0.5 β and 1.5 β, respectively. The number of generated scenarios by sampling from the Gaussian PDFs is 10,000 and it is reduced to 20 scenario by backward method [49]. The final scenarios are listed in Table 1. The nominal power of wind and solar PV is 100 kW. The power generation profile of renewable resources as well as electrical and heating loading at 24 h for all of seasons are shown by Figs. 6–11.

The hourly prices of active power and NG in four seasons are depicted in Figs. 12 and 13. The price of heating curtailed power by load shedding program is 20% more than NG price. The other economic parameters and coefficients are listed in Table 2.

The shiftable and curtailable loads, participating in DRP and load shedding programs as well as critical loads are listed in Table 3. The transfer time matrix for mobile battery stations is presented by Table 4. The equipment characteristic, conversion coefficients and economic parameters are presented in Table 5. The numbers of season's days equal 90, 93, 90 and 92 and faults specification in all seasons are shown in Table 6. It is noteworthy that the test case network is small and the buses of the network are close to each other, therefor the traveled distance by the truck is not significant and the emissions of the truck are ignored in the proposed model.

5. Simulation results

The formulated MILP is solved by a personal computer with processor core i7, CPU@ 4 GHz and RAM 8 GB. The numerical results are given after solution in GAMS software under following cases:

Case 1: simulation with fixed diesel DG and fixed battery storage.

Case 2: simulation with mobile diesel DG and fixed battery storage.

Case 3: simulation with mobile diesel DG and mobile battery storage.

5.1. Comparsion of different cases

The economic outputs of the plan under different cases are summarized in Table 7. As seen in the table, mobility of diesel DG

Table 1
Scenarios details (W: wind, S: Solar PV, L: load).

Scenario	Parameter	Time interval																								Probability
		1	2	3	4	5	6	7	8	9	10	11	12	13	14	15	16	17	18	19	20	21	22	23	24	
1	W	α	A	α	α	α	α	α	α	α	α	α	α	α	α	α	α	α	α	A	α	α	α	α	α	0.1
	S	α	A	α	α	α	α	α	α	α	α	α	α	α	α	α	α	α	α	A	α	α	α	α	α	
	L	α	A	α	α	α	α	α	α	α	α	α	α	α	α	α	α	α	α	A	α	α	α	α	α	
2	W	β	B	β	β	β	β	β	β	β	β	β	β	β	β	β	β	β	β	B	β	β	β	β	β	0.19
	S	β	B	β	β	β	β	β	β	β	β	β	β	β	β	β	β	β	β	B	β	β	β	β	β	
	L	β	B	β	β	β	β	β	β	β	β	β	β	β	β	β	β	β	β	B	β	β	β	β	β	
3	W	δ	Δ	δ	δ	δ	δ	δ	δ	δ	δ	δ	δ	δ	δ	δ	δ	δ	δ	Δ	δ	δ	δ	δ	δ	0.06
	S	δ	Δ	δ	δ	δ	δ	δ	δ	δ	δ	δ	δ	δ	δ	δ	δ	δ	δ	Δ	δ	δ	δ	δ	δ	
	L	δ	Δ	δ	δ	δ	δ	δ	δ	δ	δ	δ	δ	δ	δ	δ	δ	δ	δ	δ	δ	δ	δ	δ	δ	
4	W	β	B	β	β	β	β	β	β	β	β	β	β	β	β	β	β	β	β	β	β	β	β	β	β	0.12
	S	β	B	β	β	β	β	β	β	β	β	β	β	β	β	β	β	β	β	β	β	β	β	β	β	
	L	α	A	α	α	α	α	α	α	α	α	α	α	α	α	α	α	α	α	α	α	α	α	α	α	
5	W	α	A	α	α	α	α	α	α	α	α	α	α	α	α	α	α	α	α	α	α	α	α	α	α	0.1
	S	β	B	β	β	β	β	β	β	β	β	β	β	β	β	β	β	β	β	β	β	β	β	β	β	
	L	β	B	β	β	β	β	β	β	β	β	β	β	β	β	β	β	β	β	β	β	β	β	β	β	
6	W	β	B	β	β	β	β	β	β	β	β	β	β	β	β	β	β	β	β	β	β	β	β	β	β	0.11
	S	α	A	α	α	α	α	α	α	α	α	α	α	α	α	α	α	α	α	α	α	α	α	α	α	
	L	β	B	β	β	β	β	β	β	β	β	β	β	β	β	β	β	β	β	β	β	β	β	β	β	
7	W	β	B	β	β	β	β	β	β	β	β	β	β	β	β	β	β	β	β	β	β	β	β	β	β	0.05
	S	α	A	α	α	α	α	α	α	α	α	α	α	α	α	α	α	α	α	α	α	α	α	α	α	
	L	α	A	α	α	α	α	α	α	α	α	α	α	α	α	α	α	α	α	α	α	α	α	α	α	
8	W	α	A	α	α	α	α	α	α	α	α	α	α	α	α	α	α	α	α	α	α	α	α	α	α	0.05
	S	α	A	α	α	α	α	α	α	α	α	α	α	α	α	α	α	α	α	α	α	α	α	α	α	
	L	β	B	β	β	β	β	β	β	β	β	β	β	β	β	β	β	β	β	β	β	β	β	β	β	
9	W	α	A	α	α	α	α	α	α	α	α	α	α	α	α	α	α	α	α	α	α	α	α	α	α	0.04
	S	β	B	β	β	β	β	β	β	β	β	β	β	β	β	β	β	β	β	β	β	β	β	β	β	
	L	α	A	α	α	α	α	α	α	α	α	α	α	α	α	α	α	α	α	α	α	α	α	α	α	
10	W	α	A	α	α	α	α	α	α	α	α	δ	δ	δ	δ	δ	δ	δ	δ	δ	δ	δ	δ	δ	δ	0.02
	S	δ	Δ	δ	δ	δ	δ	δ	δ	δ	β	β	β	β	β	β	β	β	β	β	β	β	β	δ	δ	
	L	β	B	β	β	β	β	β	β	β	β	β	β	α	α	α	α	α	α	α	α	δ	δ	δ	δ	
11	W	δ	Δ	δ	δ	δ	δ	δ	δ	δ	δ	δ	δ	δ	δ	δ	δ	δ	δ	δ	δ	δ	δ	δ	δ	0.02
	S	δ	Δ	δ	δ	δ	δ	δ	δ	δ	δ	δ	δ	δ	δ	δ	δ	δ	δ	δ	δ	δ	δ	δ	δ	
	L	β	B	β	β	β	β	β	β	β	β	β	β	β	β	β	β	β	β	β	β	β	β	β	β	
12	W	δ	Δ	δ	δ	δ	δ	δ	δ	δ	δ	δ	δ	δ	δ	δ	δ	δ	δ	δ	δ	δ	δ	δ	δ	0.03
	S	α	A	α	α	α	α	α	α	α	α	α	α	α	α	α	α	α	α	α	α	α	α	α	α	
	L	δ	Δ	δ	δ	δ	δ	δ	δ	δ	δ	δ	δ	δ	δ	δ	δ	δ	δ	δ	δ	δ	δ	δ	δ	
13	W	β	B	β	β	β	β	β	β	β	β	β	β	β	β	β	β	β	β	β	β	β	β	β	β	0.03
	S	δ	Δ	δ	δ	δ	δ	δ	α	α	α	α	α	α	α	α	α	δ	δ	δ	δ	δ	δ	δ	δ	
	L	δ	Δ	δ	α	α	α	α	α	α	α	α	α	α	α	δ	δ	δ	δ	δ	δ	δ	δ	δ	δ	
14	W	δ	Δ	δ	δ	δ	δ	δ	δ	δ	δ	δ	β	β	β	β	β	β	β	β	β	β	β	β	β	0.01
	S	β	B	β	β	β	β	β	β	β	β	β	β	δ	δ	δ	δ	δ	δ	δ	δ	β	β	β	β	
	L	β	B	β	δ	δ	δ	δ	δ	δ	δ	δ	β	β	β	β	δ	δ	δ	δ	δ	β	β	β	β	
15	W	δ	Δ	β	δ	δ	δ	δ	δ	β	δ	δ	β	δ	δ	δ	δ	δ	β	δ	δ	δ	δ	δ	δ	0.01
	S	δ	Δ	δ	δ	β	δ	δ	δ	β	δ	δ	δ	δ	δ	β	δ	δ	δ	δ	δ	δ	δ	δ	δ	
	L	δ	Δ	δ	δ	δ	δ	δ	β	δ	δ	δ	δ	δ	δ	δ	β	δ	δ	δ	β	δ	δ	δ	δ	
16	W	δ	B	δ	δ	β	δ	β	β	β	δ	δ	δ	α	β	β	δ	α	β	δ	δ	δ	δ	β	β	0.01
	S	δ	Δ	α	δ	α	β	δ	δ	δ	δ	δ	β	β	α	δ	δ	β	δ	α	δ	β	δ	δ	δ	
	L	δ	B	β	β	δ	δ	δ	α	α	β	β	δ	δ	δ	β	α	δ	δ	δ	β	δ	δ	β	δ	
17	W	α	A	β	β	δ	α	β	α	δ	δ	β	β	δ	β	α	δ	β	β	δ	β	δ	β	β	δ	0.01
	S	δ	A	δ	δ	α	δ	α	δ	δ	δ	α	β	δ	δ	δ	δ	δ	β	δ	δ	β	β	δ	δ	
	L	δ	B	β	α	α	δ	α	δ	δ	β	α	α	β	β	β	β	δ	β	β	β	δ	β	α	α	
18	W	δ	B	δ	α	δ	δ	β	β	δ	α	α	β	β	δ	δ	β	β	β	δ	β	δ	δ	α	β	0.02
	S	α	B	δ	α	β	β	β	β	δ	δ	δ	α	α	α	δ	α	β	β	δ	α	δ	α	α	β	
	L	δ	A	α	α	α	α	δ	α	α	α	α	β	δ	β	δ	α	δ	δ	β	β	α	α	δ	β	
19	W	α	Δ	α	δ	β	δ	α	β	δ	α	α	α	β	β	β	α	β	α	α	α	δ	β	δ	α	0.01
	S	α	A	β	β	β	β	α	β	α	β	δ	δ	α	α	α	α	β	α	β	α	β	δ	β	β	
	L	δ	B	α	β	β	δ	β	δ	α	α	α	α	β	δ	α	δ	α	δ	α	β	β	α	β	α	
20	W	β	B	δ	δ	β	α	β	β	α	β	δ	β	α	α	β	δ	β	β	β	α	α	α	δ	α	0.01
	S	β	B	β	α	β	α	α	δ	β	α	β	β	β	δ	δ	α	α	α	α	α	δ	α	β	α	
	L	β	B	β	β	β	δ	α	α	δ	α	β	β	α	α	β	δ	α	α	δ	α	β	α	α	α	
Probability summation																										1

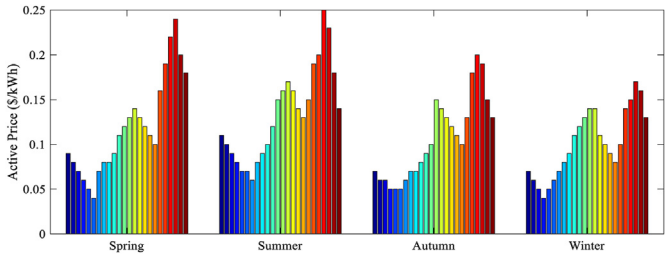

Fig. 12. Hourly energy price in four seasons.

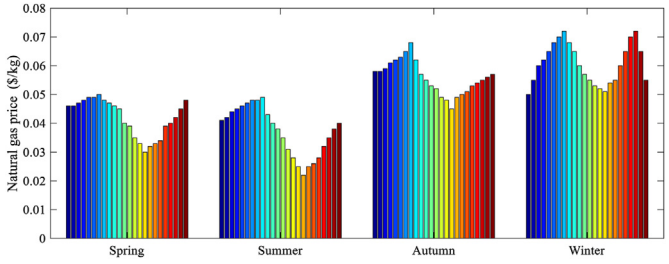

Fig. 13. Hourly NG price in four seasons.

Table 2
Coefficients of economice parameters.

Pr_q ($/kWh)	Pr_{drp} ($/kWh)	Pr_{drq} ($/kWh)	Pr_{pshed} ($/kWh)	Pr_{qshed} ($/kWh)
0.2	1.2	0.24	1.2	0.24

and battery storage can decrease all the system costs. The total cost of system is reduced by 16.5% while the other costs such as purchased energy, purchased NG and losses are decreased by 16.5%, 22.9% and 21.5%, respectively. The mobile diesel DG and battery are very effective in reduction of load shedding and penalty cost where these costs are reduced by 30.1% and 31.3%, respectively. One of the reasons of reduction in the purchased NG cost is lesser generation by CHP unit that reduces the start-up and shut down cost of CHP by 11.2%.

One of the other advantages of mobile diesel DG and battery is to increase the electrical and heating load restoration at fault times as shown by Table 8. According to this table, it is observed that the proposed model not only increases the electrical load restoration by 43% but also improves the heating load restoration by 26%. The relief of CHP capacity for more heating generation instead of electricity under fault 2 is the main reason of improving the heating

Table 4
Transfer time (hour) matrix for mobile battery storage stations.

Bus number	6	13	20	24	30
6	0	1	1	1	3
13	1	0	1	1	2
20	1	1	0	1	1
24	1	1	1	0	1
30	3	2	1	1	0

load restoration and this point is shown by Figs. 14 and 15. It is clear that at this time due to outage of NG (fault 2), the needed NG of CHP must be supplied by NG storage tank. Input-output NG to storage tank under case 3 and fault 2 is shown by Fig. 16.

The diesel DG with seasonal movement and battery storage with hourly movement can enhance the electrical and heating load supply at fault times. For example, load supply of bus 16 in electrical network and bus 5 in heating network are shown by Figs. 17 and 18, respectively. As seen in this figure, from case 1 to case 3, the system deterioration is decreased, meanwhile the self-adequacy of system is increased by 2.5 h.

5.2. Mobile battery storage assesement

The hourly behavior of mobile battery storage in four seasons and three fault states is presented in Table 9. As seen in table, under all fault states at beginning of the day, the battery is discharged in agricultural and industrial areas due to peak load of these areas, while the battery is charged at midday in the residential and agricultural areas.

Under fault 1, the battery is discharged in all seasons as well as the reactive power is generated in order to prevent the voltage drop. As seen in table, the most reactive power is generated in fault 1 to improve the voltage profile. As in was mentioned, at fault 2, the battery with more active power generation releases the CHP capacity for more heating generation and this point is shown in the column related to fault 2.

5.3. Mobile diesel DG assesement

In the given model the diesel DG moves on the buses seasonally. The diesel DG locations in different seasons is listed in Table 10. As seen in the table, the diesel DG is installed on agricultural area in the summer and it is installed on the industrial area in the other seasons. This result is reasonable because the agricultural loads are maximum in the summer as well as there are six critical loads in the industrial area that must be supplied under any conditions.

The diesel DG operation in summer is shown by Fig. 19.

Table 3
Shiftable, critical and curtailable loads.

Load type	Bus. No.	
	Electrical network	Heating network
Participating loads in DRP (Shiftable loads)	3-4-6-22-23-24	–
Critical loads	7-8-9-12-14-15	2–3
Participating loads in load shedding program (curtailable loads)	Other buses	Other buses

Table 5
Technical parameters.

Eini (kWh)	Emax (kWh)	Emin(kWh)	H^{A}_{chp}(kW)	H^{B}_{chp}(kW)	H^{C}_{chp}(kW)	H^{D}_{chp}(kW)
300	3000	10	0	600	300	0
P^{A}_{chp}(kW)	P^{B}_{chp}(kW)	P^{C}_{chp}(kW)	P^{D}_{chp}(kW)	P^{max}_{ch}(kW)	P^{max}_{dis}(kW)	Prsh ($)
1000	500	60	200	800	800	10
Prst ($)	Prpdg ($/kWh)	NG^{ini}_{tank}(kg)	NG^{max}_{rate}(kg/h))	NG^{min}_{cap}(kg)	NG^{max}_{cap}(kg)	S^{max}_{line}(kVA)
10	0.142	400	50	50	1300	4000
S^{max}_{DG}(kVA)	S^{max}_{MB}(kVA)	H^{max}_{bo}(kW)	ΔT (hour)	βNG(kg/kWh)	η^{chp}_{P}(%)	η^{chp}_{H}(%)
1300	800	1000	1	0.068	50	45
η^{bo}_{H}(%)	ηch(%)	ηdis(%)	γ	$\xi^{hh'}_{loss}$	L	
85	98	98	0.1	0.9	30	

Table 6
Fault specification in all seasons.

Seasons		Spring	Summer	Autumn	Winter
Without fault	Number of days	88	91	88	90
Fault 1 (outage of electrical grid)	Number of days	1	1	1	1
	Fault duration (hour)	13–20	13–20	13–20	13–20
Fault 2 (outage of NG grid)	Number of days	1	1	1	1
	Fault duration (hour)	1–8	1–8	1–8	1–8

Table 7
Annual costs of system under different cases.

Case No.	Purchased Energy ($/year)	Purchased NG ($/year)	Losses ($/year)	Demnad response ($/year)	Electrical load shedding ($/year)	Heating load shedding ($/year)	Diesel DG ($/year)	CHP ($/year)	Total cost ($/year)
Case1	1722876	854421	11124	15447	11245	4741	368942	6127	2994923
Case2	1575987	762437	9957	15174	10243	4137	362417	5874	2746226
Case3	1438872	658691	8733	14991	7854	3257	361396	5440	2499234

Table 8
Total load restoration under different cases.

Case No.	Load restoration (%)	
	Electrical load	Heating load
Case 1	36	25
Case2	58	37
Case3	79	51

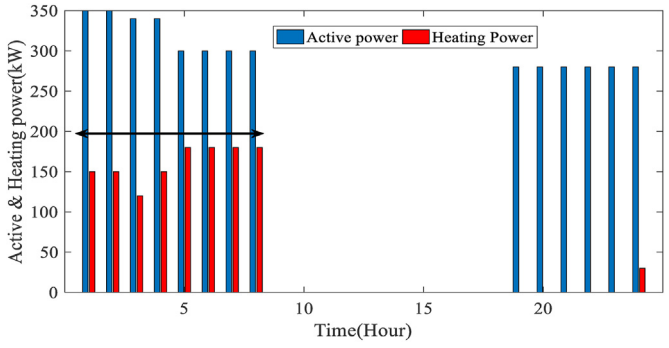

Fig. 14. CHP generation in case 1 and fault 2.

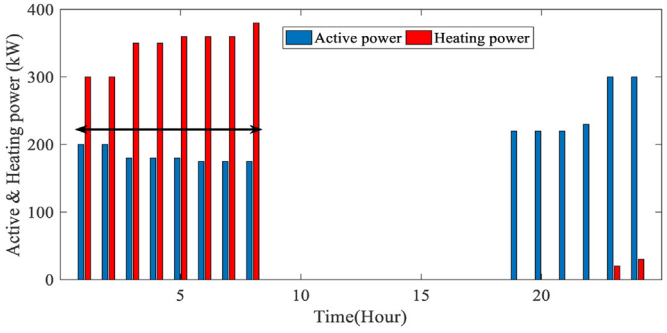

Fig. 15. CHP generation in case 3 and fault 2.

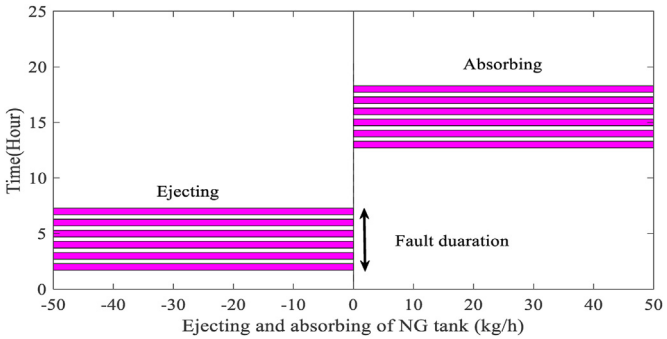

Fig. 16. Input-output NG to storage tank in case 3 and fault 2.

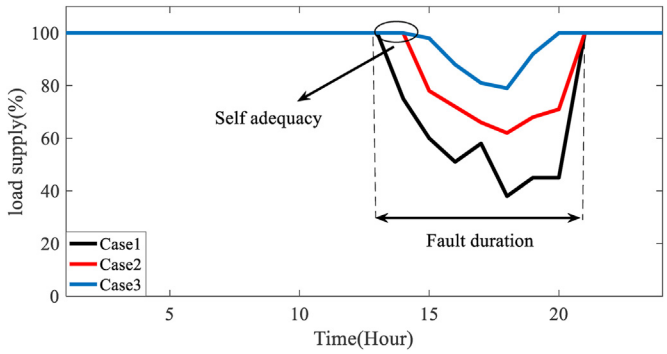

Fig. 17. Hourly supplied electrical load in bus 16 and fault 1.

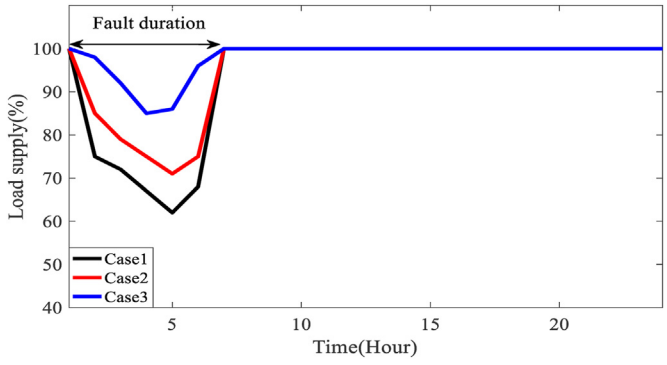

Fig. 18. Hourly supplied heating load in bus 5 and fault 2.

According to this figure, the diesel DG generates the active power in the beginning and end of day, because the agricultural loads are maximum at these hours. Generation of diesel DG in winter and fault 1 is shown by Fig. 20. As seen in the figure, under fault duration, the active and reactive generation of diesel DG is increased due to supplying the critical loads and preventing voltage drop.

Table 10
Mobile diesel DG location in different seasons.

Season	Spring	Summer	Autumn	Winter
Bus No.	8	28	8	12

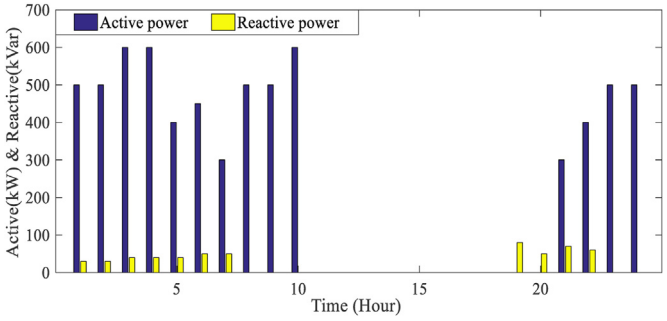

Fig. 19. Operation of mobile diesel DG in summer without fault days.

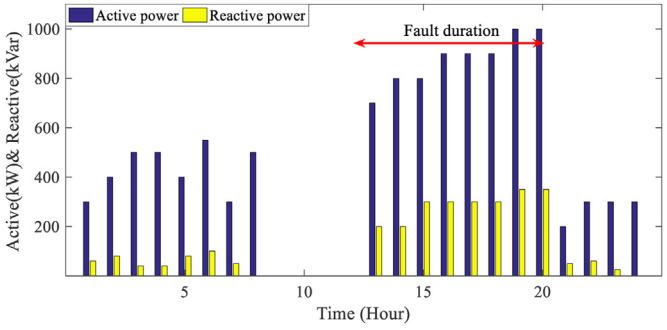

Fig. 20. Operation of mobile diesel DG in winter under fault 1.

5.4. Demand response program analysis

The participating loads in the DRP are six loads in the residential area. The shifted demand of participating buses in the DRP is listed in Table 10 in summer and fault 1. As seen in table, in order to

Table 9
Hourly operation of mobile battery storage in four seasons (**green cell**: transfer time; **yellow cell**: reactive power generation; **red number**: location of battery (bus number); **black number**: charging-discharging power (kW)).

Time	Without fault				Fault 1				Fault 2			
	Spring	Summer	Autumn	Winter	Spring	Summer	Autumn	Winter	Spring	Summer	Autumn	Winter
1	0 30	0 30	-50 13	-60 13	-60 30	-60 30	-50 13	-60 13	-30 30	-30 30	-25 13	-20 13
2	-60 30	-60 30	-0 13	-60 13	-60 30	-60 30	-50 13	-60 13	-40 30	-30 30	-25 13	-20 13
3	-60 30	-60 30	-50 13	-60 13	-60 30	-60 30	-50 13	-50 13	-50 30	-30 30	-50 13	-55 13
4	0 30	-80 30	-50 13	-60 13	-60 30	-60 30	-50 13	-50 13	-40 30	-40 30	-50 13	-55 13
5	-60 30	-80 30	-50 13	0 13	-0 30	-50 30	-50 13	0 13	-50 30	-50 30	-50 13	-60 13
6	0 30	0 30	0 13	0 13	*	*	0 13	*	-40 30	-50 30	-40 13	-40 13
7	-60 30	*	-50 13	*	500 24	500 20	*	600 20	-40 30	-60 30	-50 13	-40 13
8	*	200 24	*	*	500 24	500 20	500 20	600 20	*	*	*	*
9	200 24	200 24	*	400 30	500 24	500 20	500 20	600 20	500 24	300 20	*	*
10	200 24	200 24	200 30	400 30	500 24	500 20	500 20	500 20	500 24	300 20	400 30	500 30
11	200 24	300 24	200 30	200 30	500 24	500 20	500 20	500 20	500 24	300 20	400 30	500 30
12	200 24	300 24	300 30	200 30	*	*	*	*	500 24	300 20	400 30	450 30
13	200 24	-150 24	300 30	200 30	-300 24	-200 24	-200 6	-400 6	300 24	-200 20	400 30	450 30
14	200 24	-150 24	300 30	200 30	-300 24	-200 24	-200 6	-400 6	300 24	-200 20	400 30	200 30
15	100 24	350 24	300 30	200 30	-300 24	-300 24	-100 6	-400 6	*	300 20	200 30	300 30
16	100 24	350 24	300 30	0 30	*	-300 24	-100 6	-200 6	-300 30	300 20	200 30	200 30
17	100 24	350 24	*	*	-200 30	*	-100 6	-200 6	-300 30	300 20	*	*
18	*	*	-400 20	-300 20	-200 30	-150 30	*	*	-300 30	300 20	*	*
19	-200 30	-300 30	-400 20	-300 20	-200 30	-150 30	-200 13	-200 13	-300 30	*	-110 13	-110 13
20	-200 30	-400 30	-400 20	-300 20	-200 30	-150 30	-200 13	-200 13	-300 30	-400 30	-200 13	-300 13
21	-200 30	-400 30	*	-300 20	-200 30	-250 30	-200 13	-200 13	-210 30	-400 30	-500 13	-400 13
22	-220 30	-200 30	-150 13	*	-160 30	-200 30	-200 13	-100 13	-200 30	-400 30	-500 13	-400 13
23	-230 30	-200 30	-150 13	-200 13	-100 30	-160 30	-150 13	-100 13	-200 30	-300 30	-500 13	-600 13
24	-210 30	-180 30	-150 13	-160 13	-100 30	-150 30	-100 13	-180 13	-200 30	-210 30	-500 13	-500 13

Table 11
Shifted demand for participating buses in demand response program in summer and fault 1 (**blue cell**: demand increment (kW), **red cell**: demand reduction (kW)).

Bus. No	Time																							
	1	2	3	4	5	6	7	8	9	10	11	12	13	14	15	16	17	18	19	20	21	22	23	24
3	+5.1	+4.3	+4.5	0	0	+5.3	+5.8	+4.7	0	0	0	0	-7.2	-6.3	-2.1	0	0	-5	-5.3	-3.8	0	0	0	0
4	+10.2	+7.1	+4	+4.1	+2.8	0	0	0	0	0	0	0	-7.8	-7	-3.7	0	-5.3	-3.2	0	-1.2	0	0	0	0
6	+2.5	+1.5	+2.3	+0.4	0	0	0	0	0	0	0	0	0	-1.8	-0.8	-2.6	0	0	-1.5	-1.5	0	0	0	0
22	+4.5	+4.3	+3.8	+6	+5.3	+3.5	0	0	0	0	0	0	-3.1	-3.2	-2.4	0	0	-4.8	-6.7	-7.2	0	0	0	0
23	+6.9	+6.9	+5.4	+4	-37	0	0	0	0	0	0	0	-4	-4.5	-5.2	0	0	-2.2	-5.2	-5.8	0	0	0	0
24	+39.3	+35.6	+33.8	+30.5	+25.3	+22.3	+24.8	+27	+29	0	0	0	-35	-32	-32.3	-35.8	-30.7	-38.6	-31.6	-31.6	0	0	0	0

supply the other loads such as critical or curtailable loads, the load reduction is carried out under fault duration as well as the demand increment is done at beginning hours of the day because the residential loads are off-peak at these hours. In Table 11, the summation of blue cells is equal to summation of red cells for each bus and this point is one of the required constraints for load shifting.

5.5. Voltage profile evaluation

According to the loading profiles, the maximum electricity is consumed in the summer. Therefore, it is beneficial to evaluate the buses voltages in the summer under fault and without fault conditions. The voltage profile at 24-h in summer without fault and with fault 1 are shown by Fig. 21. The voltage levels on all busses are in the permitted range from 0.9 to 1.1 per-unit under all conditions. This point shows that the operation and location of mobile diesel DG and mobile battery storage are optimized efficiently and accurately.

5.6. Network under different faults

In order to evaluate the operation of the proposed model under various events, the network is simulated under various faults with different types and time-periods. The specifications of new applied faults are listed in Table 12. It is clear that the faults are applied in all seasons with different time-periods and types. The numerical results show that the problem is feasible under all conditions. The annual costs of system under different cases and new faults are summarized in Table 13. The total cost of system under case 3 (the proposed model) is reduced by 22.3% because with increasing number of faults, the effect of mobile battery and diesel DG in reduction of annual cost is increased. The total load restoration under different faults is shown in Table 14. According to the results, the electrical and heating load restoration are improved by 49% and 27%, respectively.

5.7. Impacts of diesel DG pollution

Total cost considering CO_2 emission cost of diesel DG is listed in

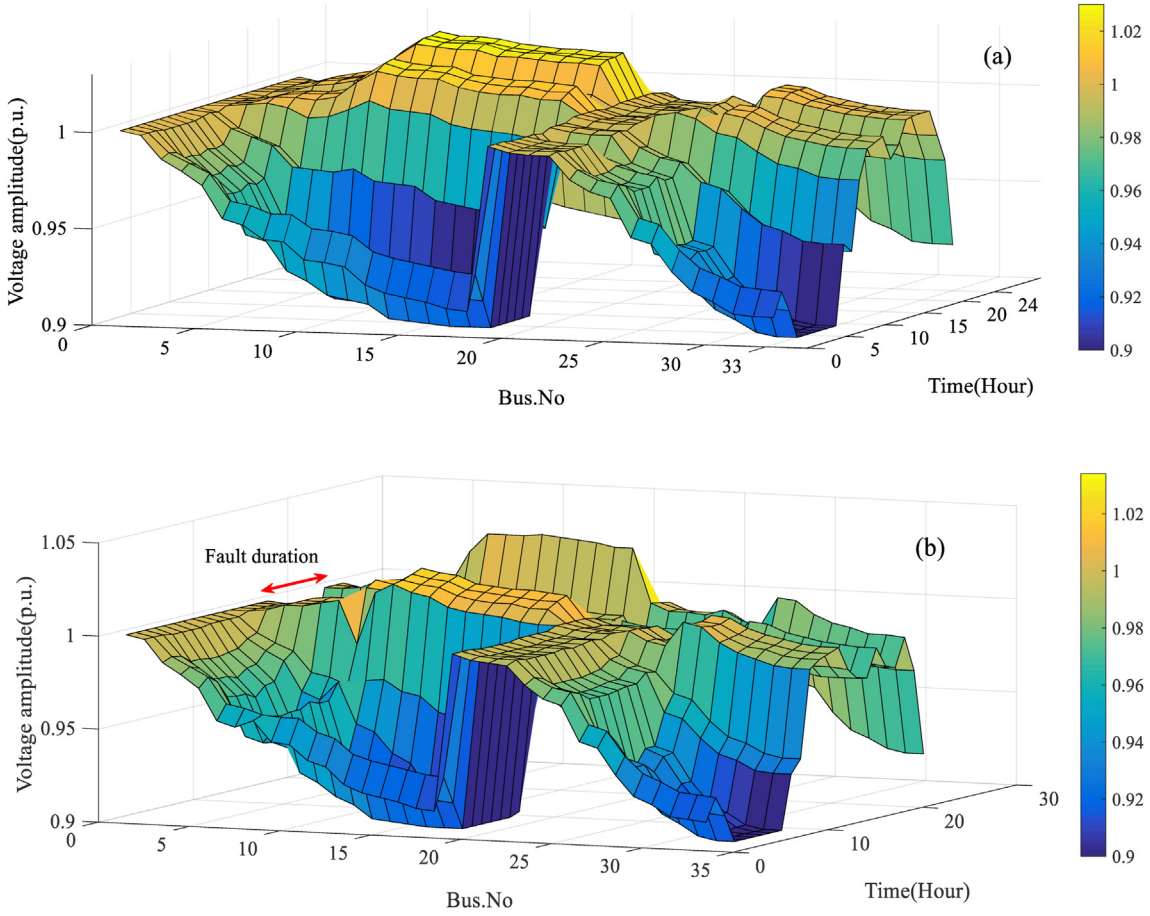

Fig. 21. Voltage profile at 24-h in summer (a) without fault and (b) with fault 1.

Table 12
Fault specifications in all seasons.

Seasons		Spring	Summer	Autumn	Winter
Without fault	Number of days	80	83	80	82
Fault 1 (outage of electrical grid)	Number of days	1	1	1	1
	Fault duration (hour)	13–20	13–20	13–20	13–20
Fault 2 (outage of NG grid)	Number of days	1	1	1	1
	Fault duration (hour)	1–8	1–8	1–8	1–8
Fault 3 (outage of Solar PV)	Number of days	1	1	1	1
	Fault duration (hour)	10–12	9–15	11–14	8–15
Fault 4 (outage of NG grid)	Number of days	1	1	1	1
	Fault duration (hour)	1–4	8–12	8–11	4–9
Fault 5 (outage of wind)	Number of days	1	1	1	1
	Fault duration (hour)	1–6	3–7	8–12	12–16
Fault 6 (outage of CHP)	Number of days	1	1	1	1
	Fault duration (hour)	23–3	20–3	8–12	11–17
Fault 7 (outage of electrical grid)	Number of days	1	1	1	1
	Fault duration (hour)	17–21	14–16	9–10	13–18
Fault 8 (outage of boiler)	Number of days	1	1	1	1
	Fault duration (hour)	15–20	15–20	22–2	10–16
Fault 9 (outage of solar PV& wind)	Number of days	1	1	1	1
	Fault duration (hour)	9–12	9–14	14–18	13–19
Fault 10 (outage of boiler)	Number of days	1	1	1	1
	Fault duration (hour)	11–13	10–12	10–15	8–12

Table 13
Annual costs of system under different cases and new faults.

Case No.	Purchased Energy ($/year)	Purchased NG ($/year)	Losses ($/year)	Demnad response ($/year)	Electrical load shedding ($/year)	Heating load shedding ($/year)	Diesel DG ($/year)	CHP ($/year)	Total cost ($/year)
Case1	2010235	964321	16789	16745	17864	9457	628745	8325	3672481
Case2	1627893	842312	12345	16012	15234	8541	512345	7425	3042107
Case3	1594882	738974	9647	15426	10274	5748	471235	6241	2852427

Table 14
Total load restoration under different cases and new faults.

Case No.	Load restoration (%)	
	Electrical load	Heating load
Case 1	20	18
Case2	41	28
Case3	69	45

Table 15. As seen in the table, the total cost of the proposed model (case 3) is less then the other cases. The conversion factors used for calculation of diesel DG emission cost can be found in Ref. [9].

6. Conclusions

This paper demonstrated the impacts of mobile battery-diesel DG in the integrated electric-heating distribution network for resilience improvement, power quality enhancement, load shedding reduction and operational cost decrease. The IEEE 33-bus electric distribution system and the 7-bus heating system were considered as case study. In order to evaluate the loading effects, the electric distribution system was divided to residential, agricultural and industrial areas with different hourly-seasonally loading profiles. The shiftable loads, curtailable loads, load shedding strategy and critical loads were considered through demand response program. The mobile diesel DG and battery were transferred on the buses seasonally and hourly, respectively. Both the active and reactive powers were considered for diesel DG, battery and CHP. For load restoration analysis, two faults were imposed on the network in each season.

The model was simulated under three cases including fixed locations for diesel DG and battery, mobile diesel DG and fixed battery and both the diesel and battery are mobile. The simulation results show that the third case (the proposed model) is more efficient because the total cost of system is reduced by 16.5% while the other costs such as purchased energy and NG, losses, DRP, electrical and heating load shedding, CHP and fuel cost of DG are decreased by 16.5%, 22.9%,21.5%, 3%, 30.1%, 31.3%, 11.2% and 2% respectively. In this case, not only the electric and heating load restoration are increased by 43% and 26% but also self-adequacy is improved almost by 2.5 h. As well, in the proposed model in order to more restoration of heating load at fault time, the active power is decreased by 40% and heating of CHP is increased by 133%. The charging-discharging of mobile battery is done at off peak and on-peak time periods, respectively in different areas. The DRP is performed correctly, because the shiftable demand is transferred to the other time-periods at fault time. Such operation causes peak shaving, cost reduction and fault effect minimization in the network. The diesel DG is installed on the industrial area due to

Table 15
Total cost considering CO_2 emission cost of diesel DG.

Case.no	Diesel DG cost ($/year)	Energy of diesel DG (kWh/year)	Generated CO_2 (kg/year)	CO_2 cost ($/year)	Total cost ($/year)
Case 1	368942	2598183	597582	1792	2996715
Case 2	362417	2552232	587013	1761	2747987
Case 3	361396	2545042	585359	1756	2500790

supply of critical loads. At the fault time, the active-reactive generation of diesel DG is increased due to supplying the critical loads and preventing voltage drop. The given model for mobile capacity resources is highly useful to increase the efficiency of resources, maximizing load restoration, enhancing self-adequacy of system, customer satisfaction, uninterrupted supply of critical loads, and reduction of total costs.

As the further works, it is suggested to consider the following items in the model and plan. The optimization problem based on the optimal selection among candidate models of facilities (e.g. types of battery, diesel DG, CHP, and tank storage) improves the optimal outputs. As well, the dynamic model of heating network as one of the practical aspects can be considered. In the large-scale electrical distribution feeders and transmission networks, the emission of the trucks is significant and had better be included in the model.

Author statement

Hasan Mehrjerdi: Supervision, Writing - Review & Editing Writing - Original Draft, Conceptualization, Methodology. **Sajad Mahdavi:** Writing - Review & Editing, Writing - Original Draft, Conceptualization, Methodology. **Reza Hemmati:** Writing - Review & Editing, Validation, Conceptualization.

Declaration of competing interest

The authors declare that they have no known competing financial interests or personal relationships that could have appeared to influence the work reported in this paper.

Acknowledgment

This work was supported by the National Priorities Research Program under Grant 11S-1125-170027 from the Qatar National Research Fund (a member of Qatar Foundation).

References

[1] Corsi S, Sabelli C. General blackout in Italy sunday september 28, 2003, h. 03: 28: 00. Conference General blackout in Italy sunday september 28, 2003, h. 03: 28: 00. IEEE, p. 1691-1702.
[2] Zetter K. Inside the cunning, unprecedented hack of Ukraine's power grid. Wired Magazine 2016;3.
[3] Operator AEM. Black system south Australia 28 september 2016. Report of the Australian energy market operator limited. AEMO); 2017.
[4] Saboori H, Hemmati R, Ghiasi SMS, Dehghan S. Energy storage planning in electric power distribution networks—A state-of-the-art review. Renew Sustain Energy Rev 2017;79:1108—21.
[5] Bao M, Ding Y, Sang M, Li D, Shao C, Yan J. Modeling and evaluating nodal resilience of multi-energy systems under windstorms. Appl Energy 2020;270:115136.
[6] Di Somma M, Graditi G, Heydarian-Forushani E, Shafie-khah M, Siano P. Stochastic optimal scheduling of distributed energy resources with renewables considering economic and environmental aspects. Renew Energy 2018;116:272—87.
[7] Mongibello L, Bianco N, Caliano M, Graditi G. Influence of heat dumping on the operation of residential micro-CHP systems. Appl Energy 2015;160:206—20.
[8] Bornapour M, Hemmati R, Pourbehzadi M, Dastranj A, Niknam T. Probabilistic optimal coordinated planning of molten carbonate fuel cell-CHP and renewable energy sources in microgrids considering hydrogen storage with point estimate method. Energy Convers Manag 2020;206:112495.
[9] Ma T, Wu J, Hao L. Energy flow modeling and optimal operation analysis of the micro energy grid based on energy hub. Energy Convers Manag 2017;133:292—306.
[10] He L, Lu Z, Zhang J, Geng L, Zhao H, Li X. Low-carbon economic dispatch for electricity and natural gas systems considering carbon capture systems and power-to-gas. Appl Energy 2018;224:357—70.
[11] Wang Y, Wang Y, Huang Y, Yang J, Ma Y, Yu H, et al. Operation optimization of regional integrated energy system based on the modeling of electricity-thermal-natural gas network. Appl Energy 2019;251:113410.
[12] Mehrjerdi H, Hemmati R. Energy and uncertainty management through domestic demand response in the residential building. Energy 2020;192:116647.
[13] Kazemdehdashti A, Mohammadi M, Seifi A, Rastegar M. Stochastic energy management in multi-carrier residential energy systems. Energy 2020:117790.
[14] Cheng Y, Zhang N, Zhang B, Kang C, Xi W, Feng M. Low-carbon operation of multiple energy systems based on energy-carbon integrated prices. IEEE Transactions on Smart Grid 2019;11(2):1307—18.
[15] Eladl AA, El-Afifi MI, Saeed MA, El-Saadawi MM. Optimal operation of energy hubs integrated with renewable energy sources and storage devices considering CO2 emissions. Int J Electr Power Energy Syst 2020;117:105719.
[16] Shabani MJ, Moghaddas-Tafreshi SM. Fully-decentralized coordination for simultaneous hydrogen, power, and heat interaction in a multi-carrier-energy system considering private ownership. Elec Power Syst Res 2020;180:106099.
[17] Mostafa Nosratabadi S, Hemmati R, Bornapour M, Abdollahpour M. Economic evaluation and energy/exergy analysis of PV/Wind/PEMFC energy resources employment based on capacity, type of source and government incentive policies: case study in Iran. Sustainable Energy Technologies and Assessments 2021;43:100963.
[18] Lei S, Chen C, Zhou H, Hou Y. Routing and scheduling of mobile power sources for distribution system resilience enhancement. IEEE Transactions on Smart Grid 2018;10(5):5650—62.
[19] Kim J, Dvorkin Y. Enhancing distribution system resilience with mobile energy storage and microgrids. IEEE Transactions on Smart Grid 2018;10(5):4996—5006.
[20] The business case for mobile batteries in New York. www.greentechmedia.com/.
[21] Department of Energy. Global energy storage database [online]. http://www.energystorageexchange.org/projects/153.
[22] Samara S, Shaaban MF, Osman AH. Optimal management of mobile energy generation and storage systems. IEEE Access 2020;8:203890—900.
[23] Sun Y, Li Z, Shahidehpour M, Ai B. Battery-based energy storage transportation for enhancing power system economics and security. IEEE Transactions on Smart Grid 2015;6(5):2395—402.
[24] Sun Y, Zhong J, Li Z, Tian W, Shahidehpour M. Stochastic scheduling of battery-based energy storage transportation system with the penetration of wind power. IEEE Transactions on Sustainable Energy 2016;8(1):135—44.
[25] Abdeltawab HH, Mohamed YA-RI. Mobile energy storage scheduling and operation in active distribution systems. IEEE Trans Ind Electron 2017;64(9):6828—40.
[26] Dong C, Gao Q, Xiao Q, Chu R, Jia H. Spectrum-domain stability assessment and intrinsic oscillation for aggregated mobile energy storage in grid frequency regulation. Appl Energy 2020;276:115434.
[27] Taheri B, Safdarian A, Moeini-Aghtaie M, Lehtonen M. Distribution system resilience enhancement via mobile emergency generators. IEEE Trans Power Deliv Aug 2021;36(4):2308—19.
[28] Yao S, Wang P, Zhao T. Transportable energy storage for more resilient distribution systems with multiple microgrids. IEEE Transactions on Smart Grid 2018;10(3):3331—41.
[29] Chen Y, Zheng Y, Luo F, Wen J, Xu Z. Reliability evaluation of distribution systems with mobile energy storage systems. IET Renew Power Gener 2016;10(10):1562—9.
[30] Song Y, Liu Y, Wang R, Ming M. Multi-objective configuration optimization for isolated microgrid with shiftable loads and mobile energy storage. IEEE Access 2019;7:95248—63.
[31] Zheng Y, Meng K, Luo F, Qiu J, Zhao J. Optimal integration of MBESSs/SBESSs in distribution systems with renewables. IET Renew Power Gener 2018;12(10):1172—9.
[32] Ebadi R, Yazdankhah AS, Mohammadi-Ivatloo B, Kazemzadeh R. Coordinated power and train transportation system with transportable battery-based energy storage and demand response: a multi-objective stochastic approach. J Clean Prod 2020;275:123923.
[33] Siddique MB, Thakur J. Assessment of curtailed wind energy potential for off grid applications through mobile battery storage. Energy 2020:117601.
[34] Saboori H, Jadid S. Optimal scheduling of mobile utility-scale battery energy storage systems in electric power distribution networks. Journal of Energy Storage 2020;31:101615.
[35] Prabawa P, Choi D-H. Multi-agent framework for service restoration in distribution systems with distributed generators and static/mobile energy storage systems. IEEE Access 2020;8:51736—52.
[36] Huang D, Chen B, Huang T, Fang X, Zhang H, Cao J. Open capacity enhancement model of medium voltage distribution network with mobile energy storage system. IEEE Access 2020;8:205061—70.
[37] Lei S, Wang J, Chen C, Hou Y. Mobile emergency generator pre-positioning and real-time allocation for resilient response to natural disasters. IEEE Transactions on Smart Grid 2016;9(3):2030—41.
[38] Abdeltawab H, Mohamed YA-RI. Mobile energy storage sizing and allocation for multi-services in power distribution systems. IEEE Access 2019;7:176613—23.
[39] Saboori H, Jadid S, Savaghebi M. Optimal management of mobile battery energy storage as a self-driving, self-powered and movable charging station to promote electric vehicle adoption. Energies 2021;14(3):736.
[40] Yang J, Zhang N, Botterud A, Kang C. On an equivalent representation of the dynamics in district heating networks for combined electricity-heat operation. IEEE Trans Power Syst 2019;35(1):560—70.
[41] Pan Z, Wu J, Sun H, Guo Q, Abeysekera M. Quasi-dynamic interactions and

security control of integrated electricity and heating systems in normal operations. CSEE Journal of Power and Energy Systems 2019;5(1):120–9.
[42] Mehrjerdi H. Resilience-robustness improvement by adaptable operating pattern for electric vehicles in complementary solar-vehicle management. Energy Storage 2021;37:102454.
[43] Nojavan S, Saberi K, Zare K. Risk-based performance of combined cooling, heating and power (CCHP) integrated with renewable energies using information gap decision theory. Appl Therm Eng 2019;159:113875.
[44] Yuan Z, He S, Alizadeh Aa, Nojavan S, Jermsittiparsert K. Probabilistic scheduling of power-to-gas storage system in renewable energy hub integrated with demand response program. Journal of Energy Storage 2020;29:101393.
[45] Santos SF, Fitiwi DZ, Shafie-Khah M, Bizuayehu AW, Cabrita CM, Catalão JP. New multistage and stochastic mathematical model for maximizing RES hosting capacity—Part I: problem formulation. IEEE Transactions on Sustainable Energy 2016;8(1):304–19.
[46] Zhang H, Heydt GT, Vittal V, Quintero J. An improved network model for transmission expansion planning considering reactive power and network losses. IEEE Trans Power Syst 2013;28(3):3471–9.
[47] Zhang H, Vittal V, Heydt GT, Quintero J. A mixed-integer linear programming approach for multi-stage security-constrained transmission expansion planning. IEEE Trans Power Syst 2011;27(2):1125–33.
[48] Baran ME, Wu FF. Network reconfiguration in distribution systems for loss reduction and load balancing. IEEE Power Eng Rev 1989;9(4):101–2.
[49] Bornapour M, Hooshmand R-A, Khodabakhshian A, Parastegari M. Optimal stochastic scheduling of CHP-PEMFC, WT, PV units and hydrogen storage in reconfigurable micro grids considering reliability enhancement. Energy Convers Manag 2017;150:725–41.